Steppe-tundra composition and deglacial floristic turnover in interior Alaska revealed by sedimentary ancient DNA (*seda*DNA)

Charlotte L. Clarke [a,1], Peter D. Heintzman [b,c,d], Youri Lammers [d], Alistair J. Monteath [e], Nancy H. Bigelow [f], Joshua D. Reuther [g,h], Ben A. Potter [h], Paul D.M. Hughes [a], Inger G. Alsos [d], Mary E. Edwards [a,f,*]

[a] *School of Geography and Environmental Science, University of Southampton, UK*
[b] *Department of Geological Sciences, Stockholm University, Stockholm, Sweden*
[c] *Centre for Palaeogenetics, Stockholm, Sweden*
[d] *The Aurora Centre for Arctic Ecosystem Genomics, The Arctic University of Norway, Tromsø, Norway*
[e] *British Antarctic Survey, Natural Environment Research Council, Cambridge, UK*
[f] *Alaska Quaternary Center, University of Alaska, Fairbanks, USA*
[g] *University of Alaska Museum of the North, Department of Anthropology, University of Alaska Fairbanks, USA*
[h] *Department of Anthropology, University of Alaska Fairbanks, USA*

ARTICLE INFO

ABSTRACT

When tracing vegetation dynamics over long timescales, obtaining enough floristic information to gain a detailed understanding of past communities and their transitions can be challenging. The first high-resolution sedimentary DNA (*seda*DNA) metabarcoding record from lake sediments in Alaska—reported here—covers nearly 15,000 years of change. It shows in unprecedented detail the composition of late-Pleistocene "steppe-tundra" vegetation of ice-free Alaska, part of an intriguing late-Quaternary "no-analogue" biome, and it covers the subsequent changes that led to the development of modern spruce-dominated boreal forest. The site (Chisholm Lake) lies close to key archaeological sites, and the record throws new light on the landscape and resources available to early humans. Initially, vegetation was dominated by forbs found in modern tundra and/or subarctic steppe vegetation (e.g., *Potentilla, Draba, Eritrichium, Anemone patens*), and graminoids (e.g., *Bromus pumpellianus, Festuca, Calamagrostis, Puccinellia*), with *Salix* the only prominent woody taxon. Predominantly xeric, warm-to-cold habitats are indicated, and we explain the mixed ecological preferences of the fossil assemblages as a topo-mosaic strongly affected by insolation load. At ca. 14,500 cal yr BP (calendar years before C.E. 1950), about the same time as well documented human arrivals and coincident with an increase in effective moisture, *Betula* expanded. Graminoids became less abundant, but many open-ground forb taxa persisted. This woody-herbaceous mosaic is compatible with the observed persistence of Pleistocene megafaunal species (animals weighing ≥44 kg)—important resources for early humans. The greatest taxonomic turnover, marking a transition to regional woodland and a further moisture increase, began ca. 11,000 cal yr BP when *Populus* expanded, along with new shrub taxa (e.g., *Shepherdia, Eleagnus, Rubus, Viburnum*). *Picea* then expanded ca. 9500 cal yr BP, along with shrub and forb taxa typical of evergreen boreal woodland (e.g., *Spiraea, Cornus, Linnaea*). We found no evidence for *Picea* in the late Pleistocene, however. Most taxa present today were established by ca. 5000 cal yr BP after almost complete taxonomic turnover since the start of the record (though *Larix* appeared only at ca. 1500 cal yr BP). Prominent fluctuations in aquatic communities ca. 14,000–9,500 cal yr BP are probably related to lake-level fluctuations prior to the lake reaching its high, near-modern depth ca. 8,000 cal yr BP.

---

1. Introduction

Interest in the full-glacial (ca. 25,000–15,000 cal yr BP) landscape and vegetation of far-northern, largely unglaciated regions, which were open and herb-dominated, has inspired palaeoecological studies since the 1960's, particularly in eastern Beringia (e.g., Colinvaux, 1964; Ager, 1975; Cwynar, 1982; Anderson et al., 2004; Zazula et al., 2007; Mann et al., 2019; Monteath et al., 2023). At a time when most other northern high-latitude regions were covered by extensive ice sheets, greater Beringia comprised an unglaciated area extending from west of the Kolyma River eastward across the exposed Bering Land Bridge into Alaska-Yukon to the limit of the Cordilleran-Laurentide ice sheet complex in Canada (Hopkins, 1982; Dyke et al., 2002; Clark et al., 2009; Hughes et al., 2016). This region provided both a refuge and a centre of diversity for the high-latitude flora (Hultén, 1937; Murray et al., 1983; Ritchie, 1984), particularly arctic-alpine taxa, but also steppe and boreal taxa (Swanson, 2002; Abbott and Brochmann, 2003; Edwards et al., 2018). How the ecosystem responded to end-Pleistocene climate warming is of particular interest, given current pressures on northern ecosystems due to rapid environmental change (Myers-Smith et al., 2011; Monteath et al., 2021).

The nature of the full-glacial vegetation and the compositional changes that occurred during the transitional period from Pleistocene to Holocene also form a critical environmental context in the story of the megafauna; the period ca. 15,000–10,000 cal yr BP saw both turnover and extinction in the mammalian fauna (Guthrie, 1990, 2006; Mann et al., 2013; Monteath et al., 2021 and references therein). Ecosystem changes, such as a shift to greater cover by woody taxa, plus changing populations of megafauna taxa, would also have affected resource use of early human populations, which entered the region at a transition from open to more woody-dominated landscapes shortly before 14,000 cal yr BP (Potter et al., 2017). In pollen records, the expansions, over a one- or two-century period, of *Betula* (ca. 14,000 years ago) and *Picea* (ca. 10, 000) years ago, which represent successive transformations of Beringian landscapes, both suggest rapid vegetation adjustments, probably to major climate shifts.

Knowledge of past flora and vegetation has been limited by available techniques. The abundant (anemophilous) pollen of dominant woody taxa and variable pollen-taxonomic resolution in most records of past vegetation masks the full extent of taxonomic turnover in the non-woody flora, and speciose plant macrofossil localities are, unfortunately, rare. This problem can be potentially addressed by a reconstruction technique that samples a relatively large, but spatially defined area—a hydrologic catchment—and resolves floristic detail, namely, sedimentary ancient DNA (*sed*aDNA) metabarcoding of lake sediments (see below). To this end, we analysed *sed*aDNA from Chisholm (also called Lost) Lake in the Tanana River Valley (Fig. 1) for the past ca. 15,300 cal yr BP with the following aims: i) obtain a detailed floristic record of late-glacial herbaceous vegetation and interpret this in terms of palaeo-vegetation communities, ii) examine in more detail than previously possible floristic and functional plant turnover from late-glacial to Holocene and its relation to environmental changes, and iii) place
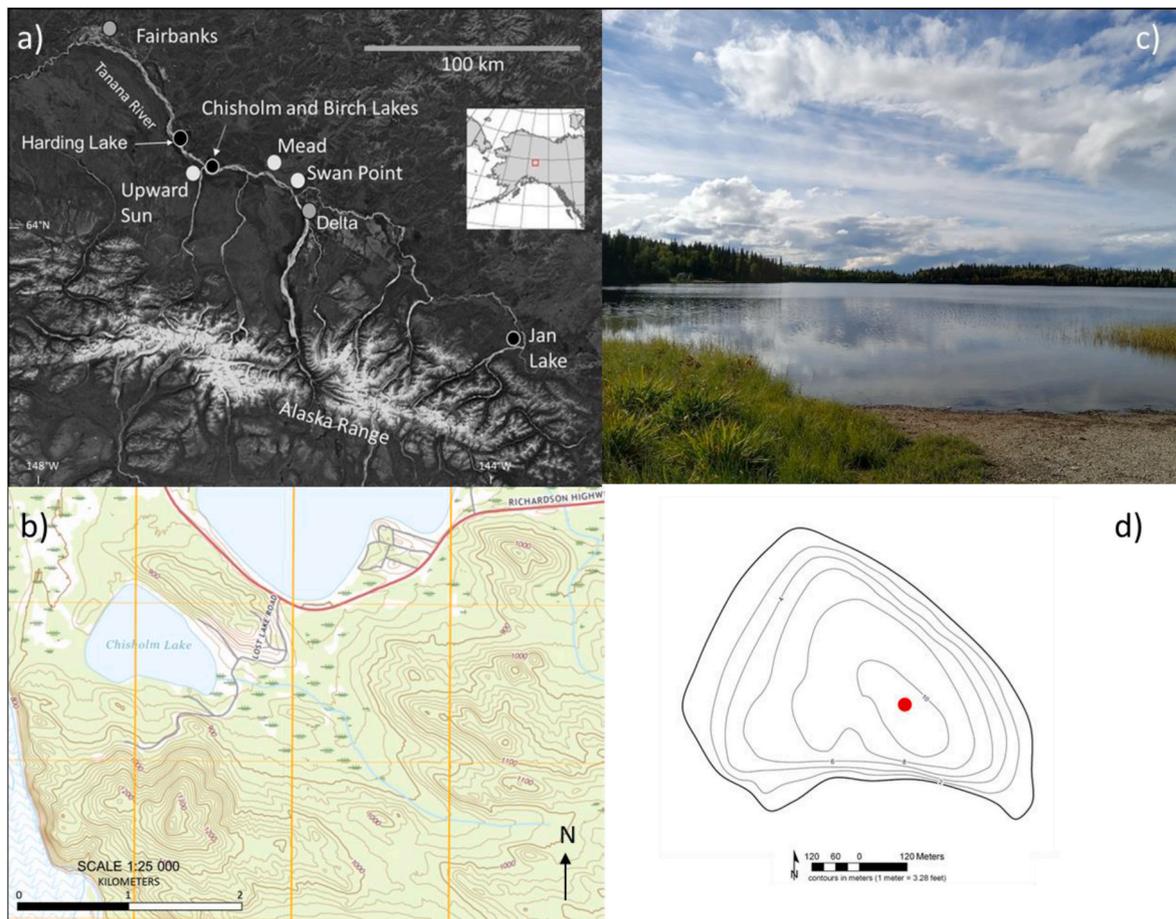
Fig. 1. a) Location of Chisholm Lake within Alaska (inset) and in the Tanana River Valley of interior Alaska, and locations of the settlements of Fairbanks and Delta. Archaeological sites are shown as white circles and lakes mentioned in text as black circles. b) Topographic map (Big Delta quadrangle, 7.5-min series) showing Chisholm Lake (Lost Lake in Tinner et al., 2006); southern tip of Birch Lake to north; Tanana River floodplain (blue wavy lines) to west; Richardson Highway shown in red. Contour interval is 20 feet. c) Looking west from the eastern shore to the location of the intermittent outlet. d) Bathymetric map of the lake basin with 2-m contours, from Alaska Department of Fish and Game (http://www.adfg.alaska.gov). The dot marks the approximate Chis 17A-B coring site (see below).

findings in the context of the landscapes encountered by humans and megafauna at the end of the Pleistocene.

1.1. Steppe, tundra, or steppe-tundra?

The nature of Beringian cold-stage treeless vegetation has been widely discussed (e.g., Colinvaux, 1964; Guthrie, 1982; Cwynar and Ritchie, 1980; Ritchie, 1984; Anderson et al., 2004). Full- and late-glacial vegetation has no strong modern pollen analogue (Anderson et al., 1989), but fossil records indicate it most likely comprised floristic and structural elements of both steppe and herbaceous tundra. For example, based on modern Alaskan distributions, prostrate *Salix* and the dwarf shrub *Arctous* indicate tundra, as do forbs such as *Draba*, *Papaver* and *Pedicularis*. Speciose grass genera, such as *Festuca*, *Poa,* and *Agrostis*, and other forb genera (e.g., *Plantago*, *Galium*) have representatives in both steppe and tundra, Given cold-stage vegetation covered a topographically complex region with substantial climatological gradients (Bartlein et al., 2015), several authors have argued, based on diverse pollen and macrofossil records, that there was local and regional habitat heterogeneity, with vegetation ranging from fellfield through forms of dry tundra to boreal steppe (e.g., Ritchie and Cwynar, 1982; Murray et al., 1983; Lloyd et al., 1994; Goetcheus and Birks, 2001; Kienast et al., 2001, 2005; Zazula et al., 2006a; Monteath et al., 2023). Today in interior Alaska and Yukon, elements of this past treeless mosaic are reflected in contemporary azonal facies of the vegetation, ranging from south-facing hill slopes and river bluffs in interior Alaska and the Yukon that support boreal steppe (Murray et al., 1983; Lloyd et al., 1994; Walker et al., 2001; Zazula et al., 2006a), to a rare steppe-tundra ecotone that occurs at mid elevation on south-facing mountains (Edwards and Armbruster, 1989; Lloyd et al., 1994), to alpine tundra and low-productivity fellfields on exposed uplands (Cwynar, 1982).

The term "mammoth steppe", initially coined by Guthrie (1982) to describe a no-analogue ecosystem with large grazers, is now widely used. "Steppe" is generally taken to imply (relatively) high vegetation productivity, whereas low pollen productivity is indicated by pollen accumulation rates in sites in eastern Beringia (e.g., Bigelow and Edwards, 2001). This 'productivity paradox' (Hopkins et al., 1982; Yurtsev, 2001) remains largely unresolved, as biomass (both mammalian and plant) is hard to estimate from fossil data. An ecological assessment of detailed past floristic records such as that of Ritchie and Cwynar (1982), which can now be done using molecular techniques, may go some way to constraining biomass estimates.

1.2. The potential of a sedaDNA approach

Ancient DNA extracted from sediments provides an important source of information on floristic composition and diversity; data have been shown to be consistent in relation to pollen and macrofossil records (see, for example, Alsos et al., 2016; Pedersen et al., 2016; Zimmermann et al., 2017; Clarke et al., 2020). Lake *sed*aDNA is almost entirely derived from the local hydrologic catchment and therefore avoids uncertainties of long-distance origin by wind transport, as is commonly found in pollen studies (Alsos et al., 2018, Sjögren et al., 2017). The overall higher taxonomic resolution (Parducci et al., 2017; Clarke et al., 2020) can highlight floristic patterns not discerned via pollen.

In two related *sed*aDNA studies of 242 and 535 samples, respectively, from across the circumpolar Arctic, (Willerslev et al. 2014; metabarcoding) and Wang et al. (2021; shotgun metagenomics) presented a large-scale composite of full-glacial Arctic vegetation dominated by forbs and graminoids. The samples in these studies derive largely from terrestrial settings, they reflect different sedimentary environments and temporal periods, and many represent short snapshots in time with limited spatial coverage, meaning there is, inevitably, constraint on insight into plant ecology and regional floristic/vegetation dynamics; however, the studies clearly demonstrate the power of *sed*aDNA to provide floristically rich records and to combine them with key

information on mammalian dynamics. In contrast, long, continuous *sed*aDNA records from key single sites reveal geographically precise details of temporal change. In a ca. 25,000-year record from the Polar Urals, Clarke et al. (2019) showed that taxonomic diversity increased, particularly over the deglacial period (ca. 17,000–9000 cal yr BP), and also that species were not lost from the extensive, altitudinally varied catchment through time as vegetation became more complex and heterogeneous. Rijal et al. (2021), combined multiple sites to show a similar trend of increased diversity across northern Fennoscandia after regional deglaciation.

In eastern Beringia, at two locations, *sed*aDNA studies of lake sediments both used a shotgun metagenomics approach. Graham et al. (2016) and Wang et al. (2017) traced the demise of the isolated Holocene population of woolly mammoths (*Mammuthus primigenius*) on St. Paul Island and associated environmental changes. Murchie et al. (2021a, b) used a targeted-capture technique to retrieve *sed*aDNA from multiple permafrost sites in Klondike, Yukon, to form a composite *sed*aDNA record spanning the last 30,000 years. It showed steppe-tundra vegetation giving way to woody shrub-tundra taxa between 13,500–13,200 cal yr BP, coincident with change in associated mammalian and insect faunas (Monteath et al., 2023). Nevertheless, the various applications of *sed*aDNA in the region to date lack the specific combination of landscape-scale spatial and fine temporal and taxonomic resolution provided by a high-resolution metabarcoding record from lake sediment.

2. Regional setting

2.1. Interior Alaska in the late quaternary

Today, Eastern Beringia comprises Alaska and unglaciated northwest Canada. Between 18,000 and 15,000 cal yr BP, the climate of interior Alaska was probably cooler overall (Bartlein et al., 1991, 2014) and certainly drier than present, with precipitation possibly half that of modern values (Barber and Finney, 2000). Lake levels in the Tanana Valley were extremely low; some basins may have been dry at times (Nakao and Ager, 1985; Abbott et al., 2000; Finkenbinder et al., 2014). Regionally, glaciers were restricted to the Alaska Range, plus a few, small glaciers in the Yukon-Tanana Uplands (Coulter et al., 1965; Kaufman and Manley, 2004). Deglaciation of the northern Alaska Range was early, with glaciers well up-valley by 14,600 cal yr BP (Briner et al., 2017).

With hemispheric deglaciation, a circulation switch from an anticyclone over the Laurentide ice sheet that maintained dry conditions to a more zonal, westerly flow brought higher levels of moisture (Bartlein et al., 2014) and rising lake levels (Abbott et al., 2000; Barber and Finney, 2000). Summer insolation and July temperatures peaked in the early Holocene (Kaufman et al., 2004), but the overall growing season lengthened in subsequent millennia (Bartlein et al., 2015). A transitional sequence from open to wooded vegetation ca. 14,000–8,000 cal yr BP began with expansion of structurally diverse woody taxa such as *Betula* and *Salix*, followed by *Populus*, *Picea* and *Alnus* (Anderson et al., 2004).

2.2. Modern setting

Chisholm Lake (64.30229 N, −146.68623 W) lies in the Tanana River valley at 256 m a.s.l. (Fig. 1a–d). The lake is accessible by road, and several houses and a camp are located near to the shore. Its surface area is ca. 42 ha, and the bedrock catchment area is ca. 780 ha. It is downstream of the much larger Birch Lake, in which water level is controlled by a weir. Currently, Chisholm Lake has a maximum depth of ca. 11.4 m (lake data from Alaska Department Fish & Game (ADFG), 2023; Fig. 1d). The pH is slightly greater than 7.0, the water clear, but brown (MEE pers. obs. 2022; ADFG, date unknown). The west end of the lake, where there is an intermittent outlet, is formed by a dam of outwash sand and gravel deposited by the Tanana River during the late

Pleistocene (Ager, 1975). Slow-flowing inlets drain today from the east and from the direction of Birch Lake, and the eastern drainage extends the catchment area considerably. The size of the lake and the nature of its catchment affect the taphonomy of *sed*aDNA (Giguet-Covex et al., 2019, 2023). In Norway, Alsos et al. (2018) showed that for small lakes only a few ha in extent with limited inflowing streams, the plant *sed*DNA signal mainly derives from within 50 m of the lake shore and may be dominated by within-lake biomass. Chisholm is far larger, and has an inflowing stream (see above), in which case we may expect some components of the terrestrial *sed*aDNA flux to be derived from both near-shore locations and more distant points via slope-wash and stream transport (Giguet-Covex et al., 2023).

Extensive Quaternary sand and loess deposits occur throughout the Tanana valley (Péwé, 1975). Loess drapes the bedrock slopes to the north and the higher, more extensive hills to the south (ca. 130 m above lake level), and the region is underlain by discontinuous permafrost (Jorgenson et al., 2008). Present-day climate conditions are characterised as boreal and continental, with mean July and January temperatures of 15.6 °C and −20 °C, respectively, recorded at Big Delta (305 m a.s.l., ca. 55 km SE of Chisholm Lake; Fig. 1a) for the period 1961–1990 (WorldClimate, 2012). The mean annual temperature is −2.3 °C, and mean annual precipitation 304 mm. The catchment vegetation is boreal forest, dominated by *Picea glauca* (white spruce) with *Betula neoalaskana* (tree birch), *Populus tremuloides* (aspen) and a few isolated *Larix laricina* (tamarack) trees. In the flats south of the Tanana River, where permafrost is usually close to the soil surface, *Picea mariana* (black spruce) and *Larix laricina* dominate. Fire is a major driver of disturbance (Viereck et al., 1992).

A pollen and plant-macrofossil record from the lake (Tinner et al., 2006) documents low pollen concentrations between ca. 15,000 and 13,500 cal yr BP, prior to the establishment of *Salix* and *Betula* shrub-tundra. Around 15 terrestrial plant taxa, many at a low concentration, occur within the lowermost pollen zones; Poaceae, Cyperaceae and *Artemisia* dominate, with occasional forbs such as *Potentilla*, *Bupleurum*, *Plantago canescens* and Chenopodiaceae. The pollen record from this site provides a useful baseline for assessing the floristic accuracy of the *sed*aDNA metabarcoding approach.

3. Materials and methods

3.1. Sediment retrieval and sub-sampling

Lake depth at the coring site (WGS84, 64.30229 N, −146.68623 W) was 10.5 m, as measured by a single-beam echo-sounder (Echotest II Plastimo). A 455-cm long sediment core (Chis17A-B) was retrieved in April 2017 from the winter ice surface using a Bolivia corer with 7.5-cm-diameter polycarbonate tubes for the uppermost sediments and 7.5-cm-diameter aluminium tubes for deeper sediments. For the basal sediments, a 5-cm-diameter modified Livingstone piston corer (Wright, 1967) was used. Due to logistic constraints, contiguous non-overlapping cores were taken. As this raises the possibility that material might be missing or that out-of-place material might find its way into the sediment at a core break, we avoided sampling near core breaks. Coring stopped when gravel was encountered; the lowermost retrieved sections were <10-cm long. Sediments were extruded, immediately wrapped, and placed in acrylonitrile-butadiene-styrene (ABS) pipe halves.

An exotic DNA tracer, comprising DNA extracted from a modern specimen of *Schlumbergera truncata* (Christmas cactus, family (Cactaceae)) mixed with DNA-free water (see Rijal et al., 2021), was sprayed on the surface of all coring equipment and core tubes. After retrieval of the sediments, all tubes and core sections were sealed immediately to minimise the risk of contamination by airborne or other modern environmental DNA. We did not detect tracer DNA in any of the samples analysed and conclude there was no detectable contamination from any of the equipment or core tubes used.

The core sections were transported and stored at 4 °C in the cold storage facility at the Alaska Quaternary Center, University of Alaska Fairbanks (UAF). Core sections were opened by longitudinal splitting in the summer of 2018. One half was used for subsampling, and the other half kept for archival purposes. The 4.5-m core was sub-sampled at 4-cm resolution, and 2-cm resolution within key sections of interest, within a dedicated ancient DNA clean-room facility at the University of Alaska Museum of the North (UAMN). Sterile tools, a full bodysuit, face mask and gloves were used. Following the protocol described by Parducci et al. (2017), the outer 10 mm of sediment was avoided or discarded, and a ca. 2-g subsample retrieved from inside the freshly exposed centre.

3.2. Lithology, radiocarbon dating and age-depth modelling

Upon longitudinal splitting of the core sections (see above), a basic lithostratigraphy was created from visual inspection. Subsamples of 2 cm³ were taken for loss-on-ignition (LOI) analyses at contiguous 1-cm intervals throughout the core using a volumetric sampler. Samples were weighed in crucibles, dried overnight at 100 °C and reweighed for dry weight determination, then ignited at 550 °C for 2 h, placed in a desiccator to cool to room temperature and reweighed. Total LOI was calculated as the percentage loss of dry weight after ignition (Heiri et al., 2001). Magnetic susceptibility was measured at 1-cm intervals on the archival core halves using a Bartington point sensor on a Geotek Ltd. Multi-Sensor Core Logger using a 10-s exposure time.

The preservation and abundance of plant macrofossil remains in the sediment core is poor. The individual plant remains picked for radiocarbon dating were too small for secure identification (most had a diameter of ca. 1.0 mm) and had to be combined to meet the minimum sample weight for Accelerator Mass Spectrometry (AMS) radiocarbon dating. Some were likely of aquatic origin, which introduces extra uncertainty to the age-depth model, as the radiocarbon age of aquatic macrofossils may be affected by old carbon from the catchment (Abbott and Stafford, 1996). Six samples were analysed for radiocarbon dating at the Keck-Carbon Cycle AMS Facility, University of California, Irvine in the spring of 2019. A further five samples were analysed in the summer of 2020 at the Poznań Radiocarbon Laboratory of the Adam Mickiewicz University, Poland.

We developed an age-depth model for core Chis17A-B using the northern hemisphere IntCal20 calibration curve (Reimer et al., 2020) and the OxCal v.4.4. Bayesian statistical program (Bronk Ramsey, 2009a). A P_Sequence depositional model was constructed using a General_Outlier model and a variable k parameter (Bronk Ramsey, 2008, 2009b; Bronk Ramsey and Lee, 2013). One radiocarbon date (UCIAMS-219310) was removed from the age-depth model as it caused a substantial age reversal and thus was considered unreliable (Table A1).

To reduce the chronological uncertainty caused by the limited availability of reliable macrofossils for radiocarbon dating, we produced a second, integrated age-depth model using similar methods, but multiple records. We used sharp pollen transitions (*Betula* rise and *Picea* rise) to link the Chis17A-B age-depth model with other AMS-dated records in the Tanana River Valley. New Bayesian age models were developed for Birch Lake (Bigelow, 1997), Jan Lake (Carlson and Finney, 2004) and Chisholm Lake (Tinner et al., 2006) and linked with the Chis17A-B age-depth model using the ' = ' operator (Bronk Ramsey, 2009a). Combining the chronological data allows the Bayesian models to inform each other. The timing of these rapid changes in the pollen records can reasonably be assumed consistent among sites, and any differences in timing are likely to be less than the two-sigma precision of the age-depth model (Figs. A1.1a and b).

Age and uncertainties are reported at two sigma (95.4%) uncertainty or as the median age throughout the manuscript using results from the integrated model. A further explanation of the age-depth models is available in Appendix A1. For the full OxCal code, see Supplementary File 1.

3.3. DNA extraction, amplification, library preparation and sequencing

DNA extraction followed a modified version of the Qiagen DNeasy PowerSoil® DNA Isolation Kit that included the addition of Proteinase-K and Dithiothreitol (DTT) to the cell lysis mix with Solution C1 and overnight incubation (Rijal et al., 2021). DNA was extracted from 120 sediment subsamples and 12 negative extraction controls, which contained no sediment and were used to monitor for contamination, within a dedicated ancient DNA clean-room facility in the Palaeoecology Laboratory at the University of Southampton (PLUS). Aliquots of DNA extract were then transferred to the ancient DNA facility at The Aurora Centre for Arctic Ecosystem Genomics, The Arctic University Museum of Norway, Tromsø, Norway, for *sed*aDNA metabarcoding data generation. Metabarcoding PCR amplification, PCR product pooling and purification, and sequencing protocols follow Rijal et al. (2021), unless otherwise stated. Each DNA extract and negative extraction control was independently amplified using uniquely tagged "gh" primers that amplify the *trn*L P6 loop of the plant chloroplast genome (Taberlet et al., 2007). Nine negative PCR controls, which contained no DNA template, and three positive ones (Rijal et al., 2021) were run alongside the sediment samples and negative extraction controls. Every sample and all negative controls underwent eight individual PCR replicates. Pooled and cleaned PCR products were then converted to three Illumina-compatible amplicon libraries using a modified version of the Illumina TruSeq PCR-free kit with unique dual indexes (Rijal et al., 2021). Each library was then sequenced on ~10% of a mid-output flow cell for 2 x 150 cycles on the Illumina NextSeq-550 platform at the Genomics Support Centre Tromsø (GSCT) at The Arctic University of Norway.

3.4. Sequence analysis and taxonomic assignments

Next-generation sequence data were analysed and identified using the OBITools software (Boyer et al., 2016; http://metabarcoding.org/obitools/doc/index.html) and further filtered with R v. 3.2.4. (R Development Core Team, 2016). Briefly, the paired-end reads were adapter-trimmed and merged with *SeqPrep* (https://github.com/jstjohn/SeqPrep/releases, v1.2). The merged data were demultiplexed according to the unique PCR tags with *ngsfilter* using a primer tag-sample lookup file (Supplementary File 2), and identical sequences were collapsed with *obiuniq*. Rare sequences, represented by two reads or less, and PCR errors were identified and removed with *obigrep* and *obiclean,* respectively.

Taxonomic assignments were performed using the *ecotag* program (Boyer et al., 2016) by matching sequences against a local taxonomic reference library (ArcBorBryo) comprising 815 arctic and 835 boreal vascular plant taxa, and 455 bryophytes (Sønstebø et al., 2010; Willerslev et al., 2014; Soininen et al., 2015). Sequences were then matched to a second reference library generated after running *ecopcr* (Ficetola et al., 2010) on the global EMBL database (release r143). To minimise any erroneous taxonomic assignments, only taxa with a match of 100% to a sequence in at least one of the reference libraries were retained. We further considered a taxon to be undetected in a PCR replicate if it was represented by fewer than 10 DNA reads in the entire dataset. Identified taxa were checked against the flora of Alaska (Hultén, 1968) and the Pan Arctic Flora (PAF) checklist (http://panarcticflora.org/). If a sequence identification was inconsistent across reference libraries, such sequences were checked against the NCBI BLAST database (http://www.ncbi.nlm.nih.gov/blast/) for alternative taxonomic assignments, and a biogeographically plausible taxon assigned where possible. In some cases, this meant a taxon at a higher taxonomic level was assigned.

The 0–8 PCR replicate dataset suppresses large variations in sequence read counts among samples but should nevertheless reflect the relative success of each sample. We assessed the success with which we recovered sequences of interest via the metabarcoding analytical quality (MAQ) score as described by Rijal et al. (2021). The 10 identified sequences with most reads were checked for the number of replicates in which they occurred (i.e., a top score of 1.0 reflects all 10 sequences occurred in all 8 replicates; lower scores reflect taxa missing from some replicates). We did not use the post-PCR lab controls for any data quality comparisons. Strong read-replicate concordance suggests that replicate number is linked to template abundance (Rijal et al., 2021).

Constrained clustering is typically used for objective zonation of biostratigraphic diagrams. We used a stratigraphically constrained cluster analysis (CONISS; Grimm, 1987) in TILIA (Grimm, 1992) v 3.0.1 (available at https://www.neotomadb.org/apps/tilia) with all 181 taxa (see below). To assess consistency of clustering among structural-functional groups, we also re-zoned the data for the following groups: woody, graminoids, forbs, and aquatics. The *sed*aDNA figures were made using TILIA and resemble conventional pollen diagrams, but abundance is based on 0–8 replicates per sample. Separate rarefaction of terrestrial and aquatic taxa was done on the dataset using PAST v 4.03 using default settings (Hammer et al., 2001). Original and rarefied data were used to describe changes and trends in floristic richness. The 0–8 dataset was also subject to detrended correspondence analysis in PAST to assess trends in compositional turnover (an indication of β diversity) across the record.

## 4. Results

4.1. Lithostratigraphy and chronology

The basal 5 cm of the 455-cm core were composed of sand, a 2-cm diameter pebble, and terrestrial gastropod shells (family Succineidae), suggesting fluvial or possibly colluvial material the base of the lacustrine sequence. The lower part of the core, to 225 cm, comprises minerogenic sediments differentiated into the lowermost three units (Fig. 2). Grey silty sand grades upward to silt with some laminae, both with low LOI (2–3%) and high magnetic susceptibility. Unit 3 contains slightly more organic silt. At ca. 225 cm (9200 cal yr BP) there is an abrupt transition to silty gyttja with LOI values increasing upward (up to 27%) and lower but fluctuating MS values (Unit 4). Upward to the surface, sediment properties remain relatively stable. No visible tephra deposits were observed.

The composite and independent age-depth models differ subtly during the early Holocene around the pollen-rise linkages (Fig. 2, A1.1, A1.2). The *Betula* linkage results in a younger modelled age for this depth: ca. 14,470 cal yr BP in the composite model, compared with 14,810 cal yr BP in the independent model. In contrast, the *Picea* linkage has little effect on the modelled age of the *Picea* rise itself. It does, however, result in older modelled ages (up to 470 years) for the sediments immediately above the linkage, which are loosely dated. This substantially reduces the model uncertainty around the sediment transition at 225 cm. The consistency between the composite age-depth model and the independent age-depth model at the *Picea* linkage suggests that Holocene portion of the Chisholm Lake radiocarbon chronology is not strongly affected by old carbon.

4.2. SedaDNA data quality

We obtained around 47 million raw DNA sequencing reads from 120 sediment samples, of which 32 million could be assigned to a sample (Supplementary File 3). Following post-identification filtering, 15 million reads remained, representing 167 vascular plant and 14 bryophyte taxa (Supplementary File 4). Of these 181 taxa, 45% were identified to the species level, 39% to genus and 16% to higher taxonomic levels. Most samples contained 100–200 total PCR replicates. All MAQ values were high, except for 13 problematic samples (Table A2, Supplementary File 3, and see below). Aquatic macrophytes account for up to 93% of all reads across samples and were thus treated separately for rarefied richness estimates.

Between 141 cm and 56 cm depth, 11 sediment samples failed (i.e., no plant taxa were detected by sedaDNA). Failed samples were
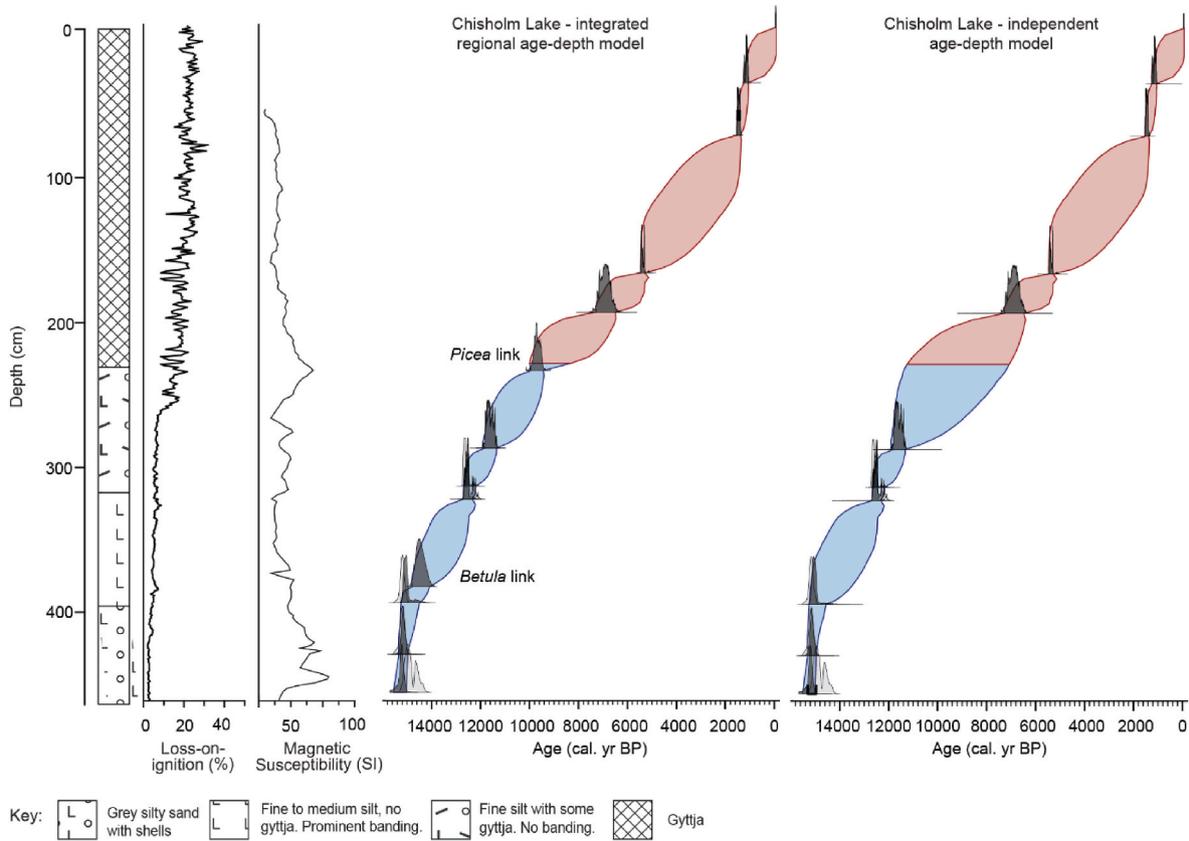
Fig. 2. Left: Lithology, loss-on-ignition, and magnetic susceptibility of the Chisholm Lake core. Middle: Age model incorporating sequences of dates tied by Picea and Betula pollen rises, from Chisholm (Lost) Lake (Tinner et al., 2006), Birch Lake (Bigelow, 1997) and Jan Lake (Carlson and Finney, 2004). Right: Age model based only on this dated core.
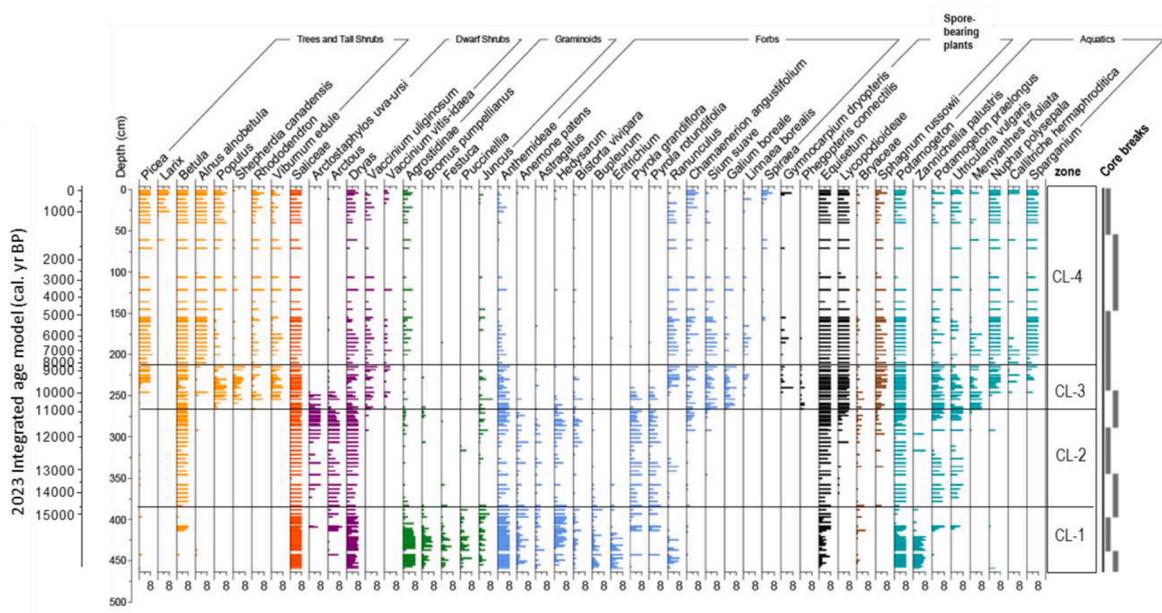
Fig. 3. Occurrence and abundance (as measured by number of PCR replicates out of eight) for key sedaDNA plant taxa at Chisholm Lake. Zones are determined by stratigraphically constrained cluster analysis (CONISS) based on abundance. Core breaks are shown to the far right. *Zone CL1 (455-383 cm; ca. 15,230–14,470 cal yr BP; herb zone).*

processed in two different DNA extraction batches that each also contained successfully amplified samples. There is no obvious explanation arising from sediment properties, data generation, or bioinformatic issues. Possibly, there was a problem with DNA extraction (e.g., inhibition that reached a lethal threshold in some samples, but not others, at this depth window). These samples were omitted from the datasets used for plotting and statistics. The continuity of the record for ca. 6000-1500 cal yr BP is somewhat compromised by these failed samples. In addition, samples at 101 cm and 350 cm had extremely low detections across all eight PCR replicates (13, 7 respectively). They were retained in plots as they nevertheless recorded the presence of multiple taxa (11, 5 respectively), but they were excluded from statistical analyses. We note that the MAQ scores for these two samples (MAQ of 0.10–0.15) are still substantially higher than the negative controls (all with MAQ of <0.07) (Supplementary File 3).

The full list of molecular taxa reported in Supplementary File 4 includes likely contaminants (e.g., common food species) and out-of-range taxa (according to Hultén, 1968). Due to sequence ambiguities, *Hulteniella* was placed in Anthemidae-2 (which includes *Achillea* and *Tanacetum*) and *Vaccinium ovalifolium* reclassified as the similar and biogeographically reasonable *V. uliginosum*.

4.3. Temporal record of floristic change

Key compositional/ecological changes for terrestrial and aquatic taxa from ca. 15,000 cal yr BP to present are summarized by a suite of key taxa (Fig. 3; Figs. A3a–d show records of all terrestrial taxa). For the sample-taxon two-way table see Supplementary File 5. Zone boundaries were defined using all taxa; boundaries defined for forbs and for aquatics separately tended to differ slightly from the all-taxon boundaries, which reflected change in tree and shrub taxa. Diagrams are plotted against depth to facilitate viewing of the early record.

Forbs and graminoids dominate the earliest period. Of all taxa identified in these groups, 54% and 78%, respectively, are detected in this zone. High values (4–8 repeats) are shown by the grass taxa Agrostidinae, *Bromus*, *Festuca*, and *Puccinellia*. Saliceae (comprising *Salix* and *Populus*), *Dryas* and *Equisetum* are abundant and present in all samples. *Potamogeton*, *Myriophyllum sibiricum*, *Stuckenia* and *Zannichellia palustris* form a distinct aquatic assemblage (Fig. 4).

Betula and several new aquatic taxa are temporarily abundant in several samples at ca. 15,100 cal yr BP (these samples are not near a core break, but they resemble coring contamination; Fig. 3). *Picea* and *Alnus alnobetula* (=*viridis*) are sporadically detected (1–2 PCR replicates).

4.3.1. Zone CL2 (383-269 cm; 14,470–11,000 cal yr BP)

Distinct and abrupt increases in *Betula* (from this point a sustained presence), *Arctous* and *Arctostaphylos uva-ursi* occur at ca. 14,470 cal yr BP. Saliceae and *Dryas* remain consistently present throughout, while *Puccinellia* and *Juncus* decrease. Previously common forbs (e.g., Anthemideae, *Anemone patens*, Asteraceae, *Potentilla*, *Pyrola* sp. and *Castilleja*) continue. Lycopods and some bryophytes appear and/or increase, including *Sphagnum russowii*. Aquatic taxon richness increases overall, although abundances of new taxa fluctuate, or taxa disappear temporarily.

4.3.2. Zone CL3 (269-215 cm; 11,000–8380 cal yr BP)

Populus increases at ca. 11,000 cal yr BP, along with a suite of shrub taxa (e.g., *Shepherdia canadensis*, *Eleagnus*, *Viburnum*, *Juniperus*) and Lycopodiaceae, plus forb taxa such as *Chamaenerion angustifolium* and *Galium boreale*. *Menyanthes trifoliata* and *Sium suave* (Figs. 3 and 4) expand at the start of the zone.

The main expansion of *Picea* occurs ca. 9600-9500 cal yr BP near the
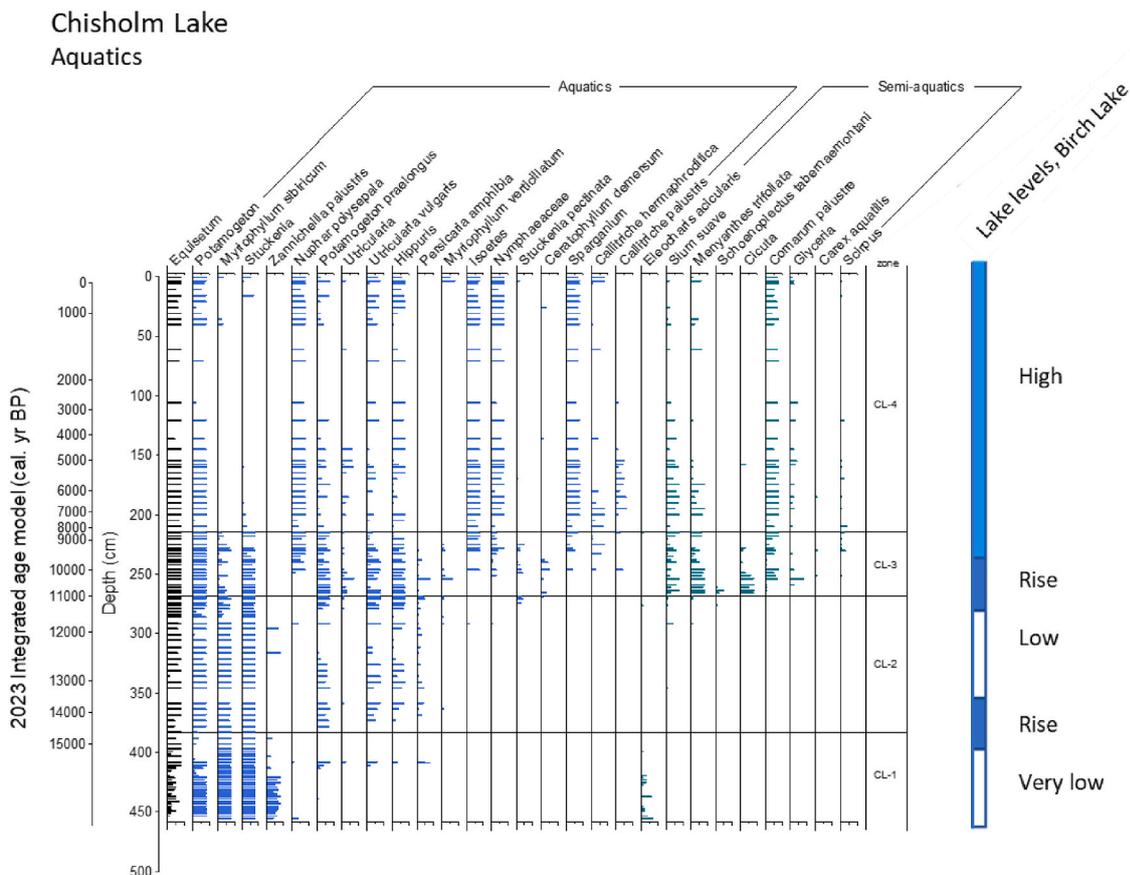
Fig. 4. Occurrence and abundance (as measured by number of PCR replicates out of eight) for key aquatic plant sedaDNA at Chisholm Lake. Birch Lake lake-level stages are on the far right. Obligate aquatic taxa are shown in blue, facultative taxa in green. Apparently thick bars reflect two or more closely spaced samples.

change to silty gyttja in the lithostratigraphy and roughly synchronous with the almost compete disappearance of *Arctous* and *Arctostaphylos uva-ursi.* Several forb taxa continuing from previous zones also decline or disappear coincident with the *Picea* rise (e.g., *Castilleja, Pedicularis, Pyrola*). *Sphagnum russowii* values increase coincident with the *Picea* rise. Aquatic taxa (e.g., *Nuphar polysepala, Isoetes, Callitriche* sp., Nymphaceae, *Sparganium*) appear or increase and become common within this zone (Fig. 4).

At 246 cm, *Picea* and *Alnus alnobetula* (=*viridis*) show high values. This sample is adjacent to a core break and the transient presence of these two taxa here probably reflects contamination (Fig. 3).

4.3.3. Zone CL4 (215-0 cm; 8380 cal yr BP to present)

The zone features a rise in *Alnus alnobetula* and *Cornus* spp., and *Ribes* and *Myrica* are consistently present. *Sphagnum russowii* (which may include other *Sphagnum* taxa) becomes abundant. Many taxa present in previous zones become rare or disappear (e.g., the dwarf shrubs, *Arctous* and *Arctostaphylos uva-ursi*, and forbs such as *Lupinus, Pedicularis*, and several Asteraceae groups), whereas new forb taxa appear (e.g., *Mertensia, Ranunculus*, Araceae and *Linnaea borealis*). Assemblages representing the period ca. 4500-1500 cal yr BP are more widely separated temporally than in other parts of the record (this section contained the failed samples). At ca. 1500 cal yr BP, *Larix* is last arboreal taxon to enter the record, but otherwise terrestrial assemblages remain compositionally similar. This zone is marked by the disappearance of the aquatics *Stuckenia* and *Myriophyllum sibiricum* (Fig. 4).

4.4. Changes in lake status and aquatic taxa

Large late-Quaternary lake-level changes reported for neighbouring Birch Lake by Abbott et al. (2000) should also have occurred in Chisholm Lake, as the two are hydrologically connected. Major shifts of aquatic taxon composition at Chisholm occur at times of recorded lake-level rise at Birch (Fig. 4). At the first rise of lake-level (at 14,500 cal yr BP, or earlier) *Zanichellia* almost disappears and *Hippuris* and *Utricularia vulgaris* join the small group of early dominants (*Potomageton, Myriophyllum sibiricum, Stuckenia*). Most notably, the second major rise to near modern levels at the onset of zone CL-3 (ca. 11,000 cal yr BP) sees the number of aquatic taxa increase further, and semi-aquatic taxa, such as *Comarum* and *Cicuta*, appear.

4.5. Relative importance of structural-functional groups

The relative number of read counts shows more clearly terrestrial taxa/functional groups that dominate the relative biomass signal or are possibly dominant for other reasons (aquatics are excluded as they represent >90% of all reads). Dominance changes over time (Fig. 5), with most groups showing a step-change in values ca. 6000 cal yr BP. Saliceae reads dominate until this point and may over-estimate its biomass contribution (see below). After the early, herb-dominated period, graminoids decline while dwarf shrubs increase, and forbs remain relatively important. Notably, the combined contribution of graminoids and forbs to total DNA reads remains as high as 30% between ca. 10,000 and 6000 cal yr BP, the early part of the forested period that is dominated by reads of trees and tall shrubs.

4.6. Diversity change

Terrestrial patterns of richness show high-frequency variability, but little overall trend. Lower values occur ca. 13,500–12,000 cal yr BP, then increase to a maximum ca. 11,000 cal yr BP, but the trends are slight (Fig. A4a). In contrast, aquatic taxa show two declines in the earlier part
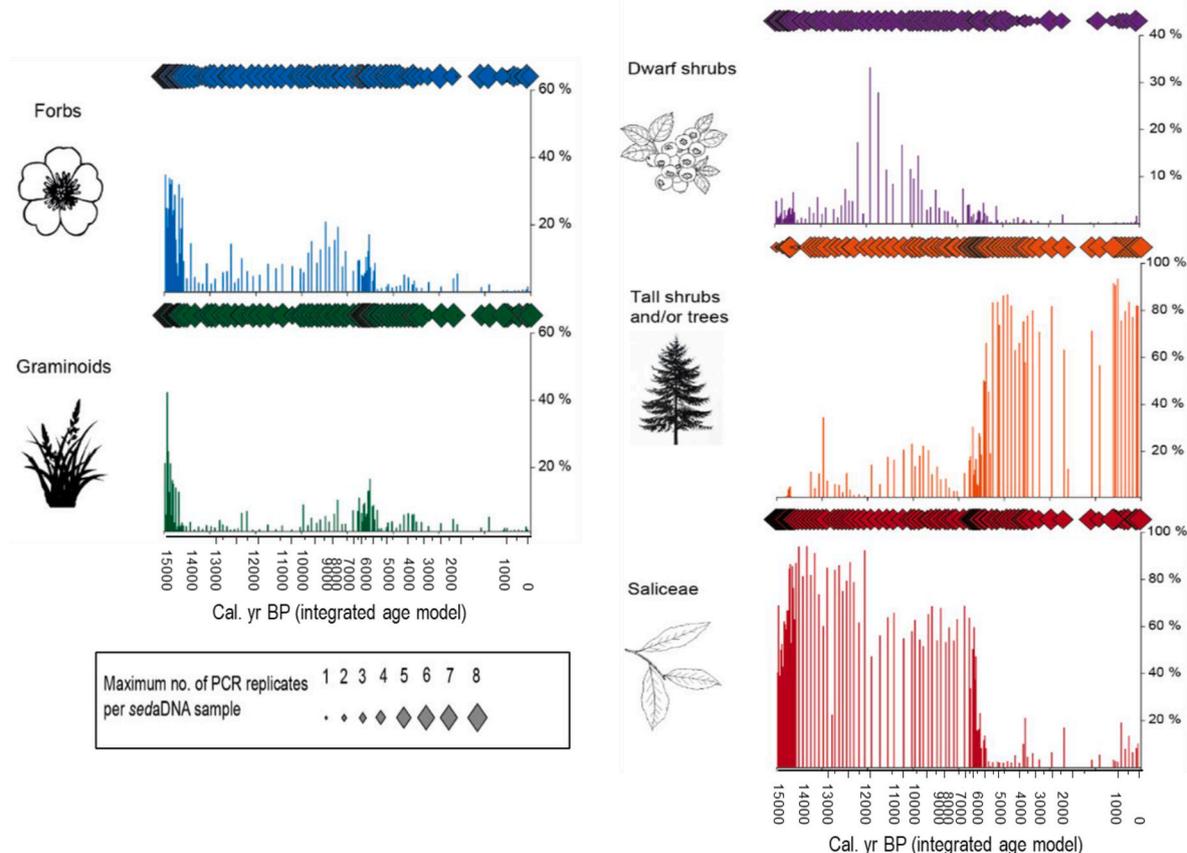

Fig. 5. Occurrence of main terrestrial structural-functional taxon groups over time at Chisholm Lake. Diamonds indicate the number of PCR replicates; bars show relative read abundance (%). Aquatic plants are not included in the calculation of relative read abundance as they comprise >90% of all reads.

of the record and peak richness ca. 7000 cal yr BP (Fig. A4b; the same pattern is retained with and without facultative aquatics). While the DCA analysis of all taxa violated the normality requirement because of skewness, as a rough guide to turnover, DCA axis one, which accounts for 52.3% of the observed variation, spans over six standard deviations (>600 units) from the earliest to latest millennia, reflecting almost complete turnover in the flora from the start to the end of the record; ca. 11,000–7000 cal yr BP was a period of particularly rapid change (Fig. A4c).

5. Discussion

5.1. General features of the Chisholm Lake record

5.1.1. Lithostratigraphy

Relatively high and primarily minerogenic sediment input early in the history of the lake is likely to reflect several processes. First, treeless vegetation would have produced little organic detritus while enhancing runoff. Second, high loess deposition rates in the Tanana valley in the late glacial and early Holocene (Péwé, 1975; Muhs et al., 2003) would have contributed airfall loess and in-washed silt. Second, greater aridity than today would have meant far lower lake levels, a reduced lake area and a relatively larger catchment area (see below and Abbott et al., 2000). The increase in sediment organic content at 225 cm (ca. 9300 cal yr BP) is likely due to rising within-lake productivity related to increasing lake volume, greater organic input linked to the spread of evergreen boreal forest (see also Bigelow, 1997) and a continuing trend of landscape-scale paludification (Mann et al., 2002; Reuther et al., 2016). That the whole section has a high in mineral component may partly explain the excellent recovery of sedaDNA, as mineral particles provide good binding sites for sedaDNA fragments (Giguet-Covex et al., 2023).

5.1.2. Quality of the sedaDNA record

Many vascular taxa were detected at Chisholm Lake throughout the record (Fig. 3 and Figs.A3a–d; Supplementary File 4). While Chisholm resembles some other long northern records in the total number of taxa identified and richness per sample (e.g., Zimmermann et al., 2017; Clarke et al., 2019), in zone 1 (herb zone), samples had high MAQ scores (0.7–1.0; Table A2), and 21–53 taxa were identified (Figs. A3a-c). This quality and richness contrasts with other records, in which the lowermost samples are often characterized by low diversity (Zimmermann et al., 2017; Alsos et al., 2021; Rijal et al., 2021). This may reflect the number of samples analysed (but all samples are rich in this zone) or unusually good preservation conditions—minerogenic sediments and a substantial catchment-lake area ratio (given a small lake) may have enhanced DNA capture and preservation (see above). It is also likely that the comparatively high per-sample richness reflects diversity inherent in eastern Beringia, which was part of a continental-scale glacial refugium (Hultén, 1937; Abbott and Brochmann, 2003, Stewart et al., 2016).

Saliceae (the poplar and willow tribe within Salicaceae) is detected in every sedaDNA sample and nearly every PCR replicate in the record, and it accounts for up to 95 % of total terrestrial DNA reads between ca. 15,000–9000 cal yr BP. Its dominance is a feature common to sedaDNA records from other northern late-Pleistocene and Holocene sites (e.g., Clarke et al., 2019; Alsos et al., 2021; Rijal et al., 2021; Murchie et al., 2021b). As it is also dominant in DNA records based on shotgun metagenomics (Wang et al., 2021), its abundance is unlikely to be related to PCR or sequencing bias. The high proportion of Saliceae and its numerical effect on read proportions supports our choice of the 0–8 abundance scale to indicate the importance of the other taxa.

5.1.3. Comparison with Chisholm (Lost) Lake pollen record

This new vascular plant sedaDNA record and the previous pollen stratigraphy of Tinner et al. (2006) from Chisholm Lake together provide an excellent opportunity to assess how sedaDNA augments and/or provides additional perspectives on the changing taxonomic composition of the late-Quaternary vegetation in interior Alaska. The overall zonation is similar; however, sedaDNA identified 60 additional terrestrial plant taxa not found as pollen, and the DNA was better able to resolve the identity of graminoids to species or genus level (Fig. A3a). Many molecular taxa also occur far more consistently than their pollen counterparts. For the earliest (herbaceous) zone, the pollen spectra are dominated by herbaceous taxa such as Poaceae, Cyperaceae, *Artemisia*, *Potentilla*, *Bupleurum*, *Plantago canescens*, Chenopodiaceae and *Equisetum*, with some *Dryas* and *Salix*, (Tinner et al., 2006), taxa also seen in the sedaDNA (Figs. A3b and c), but the sedaDNA record is floristically far richer. SedaDNA detected 48 forb taxa, most of which were not detected by pollen, likely due to low pollen productivity and/or low overall pollen concentrations (i.e., pollen sum <200 grains; 23 terrestrial plant taxa detected in total, many at <5 % of terrestrial pollen sum).

5.2. The record of terrestrial change

The sedaDNA data provide an exceptional record of floristic composition from the onset of deglaciation through the Holocene, allowing a close examination of the glacial/late-glacial herbaceous flora as it was prior to the terminal declines of now regionally extinct megafauna species and arrival of humans, and of the subsequent changes affecting landscape, vegetation and lake status that would have impacted humans and other mammals alike. While key changes that shape the pollen record—driven by the expansion of a set of woody taxa after ca. 14,470 cal yr BP—are mirrored in the sedaDNA, we can observe detail of the transitions and the turnover of numerous taxa well represented in sedaDNA but not commonly observed in pollen.

Overall, *seda*DNA records a more complex mixture of plant communities than can be interpreted from pollen, in particular, the herbaceous communities of the late glacial, the early woodland communities and the aquatics. The high number of taxa provide a robust basis for examining turnover and richness patterns as communities were replaced through time (Figure A4a and A4c). The high turnover shows that there has been replacement of taxa over time, while a relatively stable level of richness has been maintained (especially clear in the rarified curve, Fig. A4a). This differs from the post-glacial richness patterns at Lake Bolshoye Shchuchye (Polar Urals), where the large elevation gradient in the catchment (>1000m) allowed arctic-alpine taxa to move upslope as climate ameliorated and new taxa occupied lower elevations; here, richness increased with time (Clarke et al., 2019).

5.2.1. Early herbaceous communities and the nature of "steppe-tundra"

Palaeoclimatic records point to warming summer temperatures by 15,000 cal yr BP as northern hemisphere insolation increased (Kaufman et al., 2004; Bartlein et al., 1991, 2015). Aridity remained high until ca.14,000–14,500 cal yr BP (Abbott et al., 2000; Barber and Finney, 2000; Kielhofer et al., 2022). Thus, the earliest period of this record was probably particularly dry.

Key patterns are evident in Fig. 3 (Figs. A3a-d show further detail). In the earliest period before ca. 14,000 cal yr BP (zone CL-1), the lake catchment was occupied by forbs, grasses, and mat-forming plants, particularly *Dryas* and to a lesser extent, *Arctous*. *Equisetum* was abundant. While Saliceae includes *Salix* and *Populus* species, Saliceae reads are likely to represent shrub-Salix species, not trees. Prostrate forms of *Salix* can comprise a large proportion of root biomass in tundra, and their remains are abundant in a full-glacial buried soil on Seward Peninsula (Goetcheus and Birks, 2001). It is also possible that larger willow shrubs occurred in catchment watercourses.

Dominant forbs included several groups of the Asteraceae (Anthemideae, which includes *Artemisia*, *Tanacetum*, and *Achillaea*), *Anemone patens*, *Astragalus*, *Bupleurum*, *Potentilla*, *Hedysarum*, *Bistorta vivipara*, *Lupinus arcticus*, *Plantago*, *Eritrichium* and *Oxytropis*; less common taxa were *Papaver*, *Draba*, and *Suaeda* (Figs. A3b and c). Only three of the 21 graminoid taxa identified were absent from this early community;

grasses, such as Agrostidinae, *Bromus pumpellianus*, *Festuca*, and *Puccinellia*, several *Carex* taxa and *Juncus* were particularly abundant. Generally, dry-to-mesic habitats are indicated by the flora. While some forb taxa have primary tundra affinities (e.g., *Arctous*, *Papaver*, *Draba*), others are found today in tundra and on disturbed slopes or in warm, dry boreal steppe communities (*Anemone patens*, *B. pumpellianus*). Other identified genera contain species that can occur in, but are not limited to, boreal steppe, e.g., *Bupleurum triadiatum*, *Plantago cancescens*, *Hedysarum alpinum*, *Potentilla hookeriana*, and *P. pennsylvanica*). *Anticlea elegans* is indicative of boreal steppe on south-facing river bluffs in interior Alaska today (Murray et al., 1983; Edwards and Armbruster, 1989; Lloyd et al., 1994). While the grass taxa were generally identified at too high a taxonomic level to narrow down ecological affinities, the presence of arid or saline conditions is not incompatible with the occurrence of several members of Anthemideae and *Puccinellia* (Kienast et al., 2005; Willerslev et al., 2014). The catchment likely supported a mosaic of open, dry tundra communities and more steppe-like communities on dry, even arid, soils, which were possibly saline along the lake shore. Given low regional moisture, trees and shrubs may have been excluded by aridity as much as cold. While the DNA reference library used for identification, ArcBorBryo, mostly contains present-day arctic and boreal plant taxa, the Chisholm assemblages notably contain more steppic elements than other records using the same reference library (e. g., Alsos et al., 2020; Norway; Zimmermann et al., 2017; NE Siberia).

Much of the debate about the nature of steppe-tundra disappears if one considers modern landscape-scale variation in growth conditions. The complex topography of the Chisholm Lake catchment (Fig. 1b) most likely underpinned a mosaic of plant habitats during the treeless late glacial, which would have been most apparent prior to the *Betula* expansion. A range of slope-aspect combinations would have created variation in incident radiation and soil moisture (Fig. A5a). South-facing slopes abutting the north side of the lake (extending several meters lower than today due to low lake-level) would have provided a hot, dry habitat in the growing season, not dissimilar to that of boreal steppe habitats today (Murray et al., 1983; Edwards and Armbruster, 1989; Chytrý et al., 2019). Indeed, incident summer radiation would have been higher than today's, given orbital changes (Berger and Loutre, 1991). In contrast, steep, north-facing slopes south of the lake would have been far cooler and more likely to be dominated by dry tundra taxa. An indication of how strongly these topoclimates can differ is given by their equivalent latitude (EL), which is calculated based on incident radiation (Lee, 1964). In the catchment, depending upon slope and aspect, the modern SW-facing equivalent latitude can be as low as 46°N and N-facing EL > 80°N (see A5). While the effects of insolation at the ground surface will have been mitigated by air temperature, taxa with greatly differing ecological preferences could have grown in the catchment, their locations determined by topography, and, possibly, how long any winter snow patches persisted in spring. Kienast et al. (2005) report a wide range of habitat preferences in macrofossil assemblages at a locality in northern Siberia that also samples a local landscape mosaic. Today, the plant communities at the extremes of an elevation gradient on arid slopes range from steppe to tundra (Edwards and Armbruster, 1989; Lloyd et al., 1994).

More generally, this study adds to increasing evidence that the northern herbaceous floras of the full- and late-glacial periods in the North were characterised by a mixture of grasses and diverse forb taxa, as observed by Willerslev et al. (2014), Murchie et al. (2021b) and Clarke et al. (2019). Chisholm Lake's sedaDNA assemblages contain a greater forb component than is suggested by many pollen records. In metabarcoding, there may be some representational bias towards forbs (Yoccoz et al., 2012), and specific polymerases can affect taxon recovery (Nichols et al., 2018), but a more recent shotgun-metagenomics study, which avoids the biases inherent in Willerslev et al. (2014) while being based on the same sample set, shows a dominance of forbs throughout the late glacial (Wang et al., 2021). It therefore seems reasonable to assume that the biomass distribution of forbs vs. graminoids within the

lake catchment is better represented by sedaDNA than by either local or regional pollen, as pollen spectra are weighted against entomophilous forbs and towards anemophilous, widely dispersed graminoids (and *Artemisia*). A vegetation mosaic of arctic-alpine dwarf-shrub and forb communities on the one hand and grass-forb steppe on the other, plus aridity and summer growing-season temperatures lower than modern, all argue that "average" landscape productivity in the Tanana valley was patchy and climatically limited—neither as low modern dry tundra nor as high as steppe.

5.2.2. Regional expansion of woody taxa, ca.14,000 cal yr BP

At the start of zone CL-2, the expansion and steady presence of *Betula* after ca.14,000 cal yr BP marks a shift towards woody vegetation cover that occurred across much of eastern Beringia (Anderson et al., 2004). Saliceae could reflect new *Salix* taxa with larger growth forms entering the vegetation, but generally a lack of large woody remains from early in this period suggests shrub—not tree—cover (both *Betula* and *Salix* are structurally highly variable; Edwards et al., 2005). Greater moisture availability was likely the main driver, as circulation patterns changed during deglaciation, restoring a zonal airmass flow that increased moisture transport to eastern Beringia (Bartlein et al., 1991, 2014; Lora et al., 2016). The dwarf shrubs *Dryas*, *Arctostaphylos* and *Arctous* were also abundant, while many of the dominant forb taxa also persisted. *Pyrola*, *Pedicularis* and Fragariinae (probably representing *Fragaria virginiana*) increased, while some other forbs (e.g., *Suaeda*, *Eritrichium*, *Draba*) disappeared, and grasses and sedges became far less abundant (Fig. 3; Figs. A3a–c).

While new species entered the record and others declined, this transition is marked by relatively low turnover in the terrestrial flora, a pattern driven particularly by the persistence of many of the forbs that were dominant in the preceding period (Fig. 3, Fig. A3b and c), but the decline of grasses (largely represented in fewer PCR replicates per sample) suggests the herb layer changed in structure and composition. In Alaska today, herbaceous taxa typical of tundra and/or boreal steppe require high light conditions to persist (Wesser and Armbruster, 1991), so continued presence of diverse forbs suggests that the landscape remained partially open. Thus, *Betula-Salix* scrub would not have occupied the whole catchment, an important feature not revealed in pollen records. This transition, as recorded by sedaDNA, features a subtle change of vegetation cover and some hindrance to the spread of shrubs, which may have been related to still low moisture levels compared with today (Barber and Finney, 2000), plus unique regional and local geologic disturbance regimes such as high aeolian activity. Kielhofer et al. (2020) and Reuther et al. (2016) point to periods of high aeolian activity and sediment source availability for aeolian transport and sediment accumulation as a driver for maintaining patches of herbaceous vegetation into the early Holocene in the Tanana Valley. Furthermore, there may have been continued disturbance by megafauna, which remained in the region during this period (Olofsson et al., 2009; Bakker et al., 2016; Monteath et al., 2021).

5.2.3. Establishment of deciduous and then evergreen boreal forest

One of the most prominent vegetation changes in the record occurred between ca.11,000 and 10,000 cal yr BP (start of zone CL-3; Fig. 3). Populus expanded and remained consistently present thereafter, its presence as an important Holocene boreal forest component far clearer in the sedaDNA than in pollen records. Both *P. tremuloides* and *P. balsamifera* are common today in interior Alaska, and *P. tremuloides* also occurs at the edge of boreal steppe communities on dry, steep slopes (Lloyd et al., 1994). Concurrently, a suite of understorey and/or open-area shrubs appeared, forming a community resembling that of warm slopes today that are wooded or partially wooded with *P. tremuloides*, *Juniperus*, *Shepherdia*, *Elaeagnus*, and *Arctostaphylos uva-ursi* (Viereck et al., 1992 pp 93–94). Maleae (probably *Amelachier alnifolia*), *Rubus* spp., and *Viburnum* spp. were also part of this community. *Arctous* persisted and was joined by *Vaccinium uliginosum*. Lycopods

and mosses in the Polytrichaceae expanded. Many forbs already present in the catchment continued and were joined by *Chamaenerion angustifolium*, which is typical of warmer slopes and is seral after fire (Fig. 3 Figs. A3a–d). These changes in understory and field layers are far less clear in pollen records.

At about 9500 cal yr BP, a further vegetation change took place, not clearly identified by zoning, but nevertheless critical for both the terrestrial and aquatic ecosystems, namely, the expansion of *Picea*, which marks a shift to evergreen forest cover. The sedaDNA taxon *Picea* includes both *P. glauca* and *P. mariana*; the pollen record of Tinner et al. (2006) indicates that *P. glauca* originally dominated, and that *P. mariana* expanded ca. 5000 cal yr BP (according to their age model). At ca. 8300 cal yr BP (zone boundary of CL-4), there was an expansion of *Alnus*, along with the virtual disappearance of *Shepherdia*, *Eleagnus* and Maleae (*Amelanchier*). Later in the zone, many forbs that had persisted from the earlier open and partially open communities declined or disappeared, but several others appeared, indicative of a *Picea* forest field layer or wet habitats: *Mertensia paniculata*, *Geocaulon lividum*, *Linnaea borealis*, *Iris setosa*, *Caltha natans*, *Sium suave* and *Cicuta*. After the *Picea* expansion, shrubs of more moist forest habitats, such as *Chamaedaphne*, *Myrica gale* and *Spiraea*, appeared sequentially, and Ranunculaceae expanded, all of which indicates further moistening of the catchment landscape, at least near the lake shore, and possibly paludification along the valley floors of inflow drainages.

The period ca. 5000-1500 cal yr BP has low temporal resolution due to failed samples (see above), but samples that are present have high MAQ values (Table A2). Little change is apparent in the forest vegetation until the expansion of *Larix* (=*L. laricina*) in the catchment ca. 1500 years ago. Today *Larix* grows near the lake close to the eastern inflow drainage.

5.2.4. Boreal tree refugium?

Ice-free northern regions may have supported refugial populations of boreal trees during the last glacial interval (e.g. Provan and Bennett, 2008; Parducci et al., 2012a, b; but see Alsos et al., 2020). Limited genetic evidence suggests that *Picea* may have persisted within lowland areas of interior Alaska and the Yukon Territory (Anderson et al., 2006, 2011; Zazula et al., 2006) report *Picea* remains dating to ca. 27,000 cal yr BP; however, fossil evidence for local presence of *Picea* during the last glacial maximum (LGM) and late glacial within Alaska is relatively weak (Hopkins et al., 1981; Brubaker et al., 2005; Edwards et al., 2014). Sporadic occurrences of *Picea sed*aDNA early in the record (Fig. 3), prior to its establishment as a forest dominant, lead to three explanatory hypotheses: i) actual presence in the catchment, ii) derivation from pollen, and iii) lab contamination.

The *sed*aDNA patterns are mirrored in pollen records from Birch and Chisholm Lakes (Ager, 1975; Tinner et al., 2006). Furthermore, tree taxa occur in other *sed*aDNA records during periods when it is unlikely that they were present at the site (e.g., Alsos et al., 2020, Norway; Clarke et al., 2020; northern Ural Mountains). Pollen from gymnosperms can contain some chloroplast DNA; this, theoretically, could be introduced into the lake sediment matrix (Parducci et al., 2017). However, the extraction of cpDNA from fossil pollen grains has proved highly challenging (Bennett and Parducci, 2006), as it requires an additional lysis step during extraction (Kraaijeveld et al., 2015; Parducci et al., 2017). Current thinking is that DNA extracted from sediments does not derive from pollen grains (Jørgensen et al., 2012; Pedersen et al., 2016; Sjögren et al., 2017; Wang et al., 2017).

At Chisholm, *Picea*, while recorded unambiguously above 250 cm, is present sporadically in exceedingly low read abundance in PCR replicates below 250 cm (1.8%), whereas it occurs in negative controls at 2–3%. Furthermore, Alsos et al. (2020) caution that the number of controls in a single study is typically insufficient to detect low-frequency contamination with certainty. The parsimonious explanation for the sporadic occurrence of *Picea* is contamination, and so the *sed*aDNA provides no evidence of late glacial conifer persistence.

5.3. Changes in lake status and biota

Given the high read counts and proportions (>90%) of aquatic taxa, the richness of aquatic and semi-aquatic taxa (26 vascular taxa) is perhaps unsurprising. Nevertheless, the record provides an exceptional picture of changes in the aquatic macroflora (Fig. 4). Until ca. 14,000 cal yr BP, a restricted group comprising *Potamogeton*, *Myriophyllum sibiricum*, *Stuckenia* and *Zannichellia palustris* may indicate an early, pioneering assemblage, probably in clear, shallow—and possibly brackish—water (e.g., Van Vierssen, 1982). (Note: the basal sediments of nearby Birch Lake are calcareous and record substantial authigenic carbonate production; Abbott et al., 2000.) After ca. 14,000 cal yr BP, coincident with the initial Birch lake-level rise, there was some turnover (e.g., *Hippuris* and *Potomageton praelongus* appeared then later temporarily declined, while *Zanichellia* disappeared).

Taxon richness fluctuated over the next several millennia, during which lake levels fluctuated at Birch Lake. After the *Picea* rise (ca. 9500 cal yr BP), when Birch Lake rose to overflow level (Fig. 4), taxon richness approximately doubled (Fig. A4b). Subsequently, after the establishment of *Picea*, the aquatics *Myriophyllum sibiricum*, *Stuckenia*, *Persicaria amphibia* and *Ceratophyllum* declined or disappeared, but other taxa appeared. *Isoetes* suggests deeper (Edwards et al., 2000) and browner water, consistent with an increase in humic input to the sediment from a *Picea*-dominated catchment. *Nuphar* and Nymphaceae (=*Nymphaea*), and *Sparganium* typically occupy shelves with water depths <1–~3 m, and their abundance indicates that the large area of the lake currently shallower than 4 m (Fig. 1d) was under water by this time. At this point, the lake increased considerably in size and physical complexity, and both factors are likely to have driven the marked increase in richness and diversity (Fig. 4). On a broad geographic scale, in Siberia, aquatic taxon diversity is correlated positively with July temperature and negatively with conductivity (Stoof-Leichsenring et al., 2022), which is consistent with an overall growing-season length increase into the middle Holocene in Alaska (Bartlein et al., 2015); also, salinity levels would have declined with increasing lake levels. The Chisholm Lake record demonstrates that aquatic sedaDNA record can be an effective recorder of responses of a lake's macroflora to changing regional palaeohydrology and water chemistry.

5.3.1. Early human interactions with megafauna in interior Alaska

Chisholm Lake lies close to several key archaeological sites (Fig. 1a), including Upward Sun River, which contains the earliest human remains in northern North America found to date (11,500 cal yr BP; Potter et al., 2011; 2014, 2017), and other localities such as Swan Point and Mead, which record well-dated human presence by ca. 14,000 cal yr BP (Holmes, 2001). Thus, early humans entered the region on the cusp of the major environmental changes described here. At the end of the Pleistocene, human settlement systems and desirable ecological habitats were largely centred on large river valley bottomlands and adjacent upland ecotones, and they overlapped with the ranges of megafauna, including bison (*Bison* sp.), wapiti (*Cervus canadensis*), horse (*Equus ferus*), and woolly mammoth (*Mammuthus primigenius*) (Potter et al., 2011; Rowe et al., 2024). While more evidence regarding human hunting of horse and mammoth in eastern Beringia is desirable to clarify the extent of this practice, evidence from Swan Point (Fig. 1a) suggests woolly mammoth hunting occurred in the middle Tanana Valley around 14,000 years ago (Rowe et al., 2024). After ca. 13,500 cal yr BP, bison and wapiti became the preferred large-mammal subsistence resources as woolly mammoth and horse populations declined to extinction (Guthrie, 2006; Potter, 2008, Potter et al., 2011).

Topographic heterogeneity at the landscape scale likely maintained a mosaic of deciduous shrubland/woodland and open areas over a ca. 5000-yr period (ca. 14,500–9500 cal. yr. BP), during which key subsistence herbivore populations—particularly bison and wapiti—persisted in the Tanana Valley (Potter, 2008). By ca. 9500 cal yr BP, a further increase in moisture availability, expansion of *Picea glauca*

(white spruce) forest, development of thicker organic soils, and a reduction in aeolian activity (Reuther et al., 2016), coincided with significant mammalian turnover, primarily the decline of bison and wapiti and persistence of moose (Guthrie, 2006; Monteath et al., 2021). Peat and muskeg formation began and accelerated over this period (Jones and Yu, 2010). By 6000-5000 cal yr BP, there was partial replacement of *Picea glauca* forests by *P. mariana* (black spruce) forests (Anderson et al., 2004), which led to a change in fire regime (Lynch et al., 2004). This coincided with marked changes in the archaeological record: a shift from the long-term conservative cultural practices of the Denali tradition (12,500–6000 cal yr BP) to a more broad-spectrum strategy based on caribou, small mammals, and later salmon and other fish—the Northern Archaic tradition (6000-1000 cal yr BP; Holmes, 2001, 2008; Potter, 2008; Potter et al., 2023).

6. Conclusions

The *sed*aDNA record from Chisholm Lake in interior Alaska resolves the composition of late Quaternary plant communities far more effectively than pollen, particularly from the *Betula* rise onward, when pollen records become dominated by a few anemophilous pollen producers. The late-glacial herbaceous plant community was floristically diverse, and the greater insight into minor taxa afforded by the *sed*aDNA record points to the flora comprising tundra taxa and more steppic elements across a topographic (topoclimatic) mosaic. The record shows a large, distinct and sustained floristic change ca. 11,000 cal yr BP, when first *Populus* and then *Picea* became established, along with a number of other woody taxa and boreal herbs often not observed in pollen records. Additionally, *sed*aDNA affords a detailed picture of aquatic plant turnover, which in turn reflects lake-level dynamics and lake water chemistry.

The analysis of *sed*aDNA makes an important contribution towards resolving the composition of the full-glacial to late-glacial flora within ice-free northern regions. It indicates precise establishment dates of taxa in a catchment, avoiding the issue of long-distance pollen transport, and it highlights palynologically "silent" taxa, such as *Larix*, which currently have a largely undocumented history in Alaska. Furthermore, continuing developments in the field promise that expanded reconstructions of ecosystem dynamics, including other key biological groups such as vertebrates, invertebrates, and microorganisms, together with new proxies for the abiotic environment, can greatly enhance understanding of how northern ecosystems have responded to past climate change, and in turn, how these changes shaped the human environment and mammalian population dynamics.

Datasets

Raw sedaDNA sequence data are available at the European Nucleotide Archive (ENA) under BioProject accession code PRJEB74037. For the OxCal code for the age model see Supplementary File (SF)1. The primer tag-to-sample lookup file required to allow data demultiplexing is SF2. For outputs from the bioinformatic analyses, including sample metadata, raw read counts, negative control statistics, and quality control data (MAQ scores) see SF3. An annotated taxon list is available in SF4. The full sedaDNA sample/taxon two-way table (PCR replicate counts) is available in SF5.

Author contributions

CLC, MEE, NHB, PDMH, JDR and BAP contributed to the concept, study design and lake coring. CLC subsampled the sediment core, extracted the DNA and performed the PCR amplifications, picked terrestrial macrofossils for ^{14}C dating and ran the LOI and magnetic susceptibility analyses. NHB and JDR described the lithostratigraphy. CLC constructed the initial age-depth model; AJM created the regional integrated chronology and final age model. Initial bioinformatic analysis and taxonomic assignment was by YL, CLC, and PDH. Post-identification filtering, assessment and visualization of the *sed*aDNA data was performed by CLC, MEE and IGA, with ecological and biogeographic interpretations by MEE and IGA and archaeological interpretations by JDR and BAP. Figures were created by MEE, CLC, AJM and NHB. CLC wrote the first draft of the manuscript. MEE wrote a revised and expanded final draft on which all co-authors commented.

Declaration of competing interest

The authors declare that they have no known competing financial interests or personal relationships that could have appeared to influence the work reported in this paper.

Data availability

Data will be made available on request.

Appendix A. Supplementary data

Supplementary data to this article can be found online at https://doi.org/10.1016/j.quascirev.2024.108672.
Clarke et al. Appendices A1-A5.

Table A1
Radiocarbon dates. Depth is depth below sediment surface. Median age and 2σ ages are in cal yr BP. *Date excluded from age model.

Core drive number and depth within drive (cm)	Laboratory	Lab ID	Depth (cm)	Age ± 1σ (^{14}C yr. BP)	Cal median age	Cal age, 2σ

(continued on next page)

Table A1 (*continued*)

| Core drive number and depth within drive (cm)	Laboratory	Lab ID	Depth (cm)	Age ± 1σ (^{14}C yr. BP)	Cal median age	Cal age, 2σ
Chis17 surface 37–38 cm	Keck-Carbon Cycle AMS Facility, USA	UCIAMS-219312	37–38	1225 ± 25	1138	1022–1257
Chis17A D1 19–21 cm	Poznań Radiocarbon Laboratory, Poland	Poz-124407	70–71	1575 ± 30	1502	1407–1694
Chis17A D2 17–19 cm	Poznań Radiocarbon Laboratory, Poland	Poz-124449	157–158	4625 ± 35	5404	5115–5536
Chis17A D2 44–46 cm	Keck-Carbon Cycle AMS Facility, USA	UCIAMS-219309	187–188	6050 ± 160	6401	5770–6773
Chis17A D3 2–3 cm*	Keck-Carbon Cycle AMS Facility, USA	UCIAMS-219310	223–224	6455 ± 25	7379	7223–7485
Chis17A D4 1–2 cm	Poznań Radiocarbon Laboratory, Poland	Poz-124450	239–240	10080 ± 50	11404	10809–11642
Chis17A D4 36-38	Poznań Radiocarbon Laboratory, Poland	Poz-124452	274–275	10500 ± 60	12134	11849–12472
Chis17A D4 27–28 cm	Keck-Carbon Cycle AMS Facility, USA	UCIAMS-219313	314–315	10600 ± 80	11894	11011–12375
Chis17A D6 47–48 cm	Keck-Carbon Cycle AMS Facility, USA	UCIAMS-219314	378–379	12745 ± 45	15241	14908–15657
Chis17A D7 28–31 cm	Poznań Radiocarbon Laboratory, Poland	Poz-124451	394–395	12740 ± 70	15200	14822–15497
Chis17B D4 16–17 cm	Keck-Carbon Cycle AMS Facility, USA	UCIAMS-219311	448–449	12570 ± 90	15470	15092–15767

A1 Age-depth model descriptions.

The independent Chisholm age-depth model (main text Fig. 2) includes 10 radiocarbon dates and the date of coring to constrain the top of the sequence (Table A1). One radiocarbon date (UCIAMS-219310) was excluded as it caused a substantial age reversal and so was considered unreliable. A boundary was placed at 225 cm, where a sharp change in sediment properties may have influenced accumulation rates.

The integrated Bayesian age-depth model (main text Fig. 2b) uses sharp changes in pollen percentages to link Chisholm Lake with age-depth models from Lost Lake (Tinner et al., 2006), Birch Lake (Bigelow, 1997) and Jan Lake (Carlson and Finney, 2004) (Figs. A1a–d), using the ' = ' operator in OxCal v.4.4.4. (Bronk Ramsey, 2009). Lost Lake refers to a previous study of Chisholm Lake, but is described using the alternative name to avoid confusion. These lakes all lie within the Tanana River valley and prominent vegetation changes are likely to be synchronous between sites. We did not include chronology from Harding Lake, as the sampling for pollen analysis is too coarse to place the *Betula* or *Picea* rises precisely (Finkenbinder et al., 2014). Finally, we did not link Jan Lake with the integrated age-depth model using the *Betula* rise as the base of this record includes atypical lithostratigraphy and biostratigraphy, as well as substantial age reversals (Carlson and Finney, 2004.

Independent Bayesian age-depth models from Lost Lake, Birch Lake, and Jan Lake (Figs. A1.1 b, c, d, respectively) are presented by Monteath et al. (2021). The modelled ages of the *Picea* rise from the models closely overlap; however, the timing of the *Picea* rise is substantially more precise in Birch Lake and Jan Lake (Fig. A1.2). This reflects the greater number of radiocarbon dates around this interval at these sites. The modelled ages of the *Betula* rise are more variable among the different sites, which is likely to reflect the greater chronological ambiguity in each record around this time (Fig. A1.2). The precision of the *Betula* rise timing is substantially more precise in Birch Lake as this is the only record that has closely bracketing radiocarbon dates. As a result, the integrated age-depth model is largely driven by the Birch Lake chronology at this point. Despite its age (nearly 25 years), the Birch Lake record remains the best dated lake-sediment record in Interior Alaska. New dates from the site are consistent with those reported by Bigelow (1997), reaffirming the importance of this record (M. Finkenbinder, pers. comm. 2023).
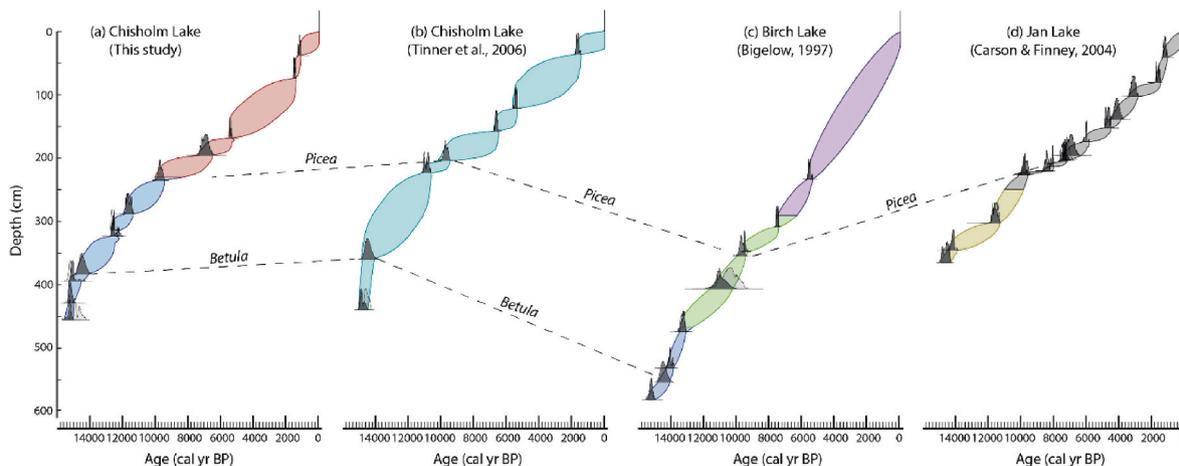
Fig. A1.1. Individual age models from (a) Chisholm Lake (this study), (b) Lost Lake (Tinner et al., 2006), (c) Birch Lake (Bigelow, 1997) and (d) Jan Lake (Carlson and Finney, 2004). Tie points are shown by dotted lines.
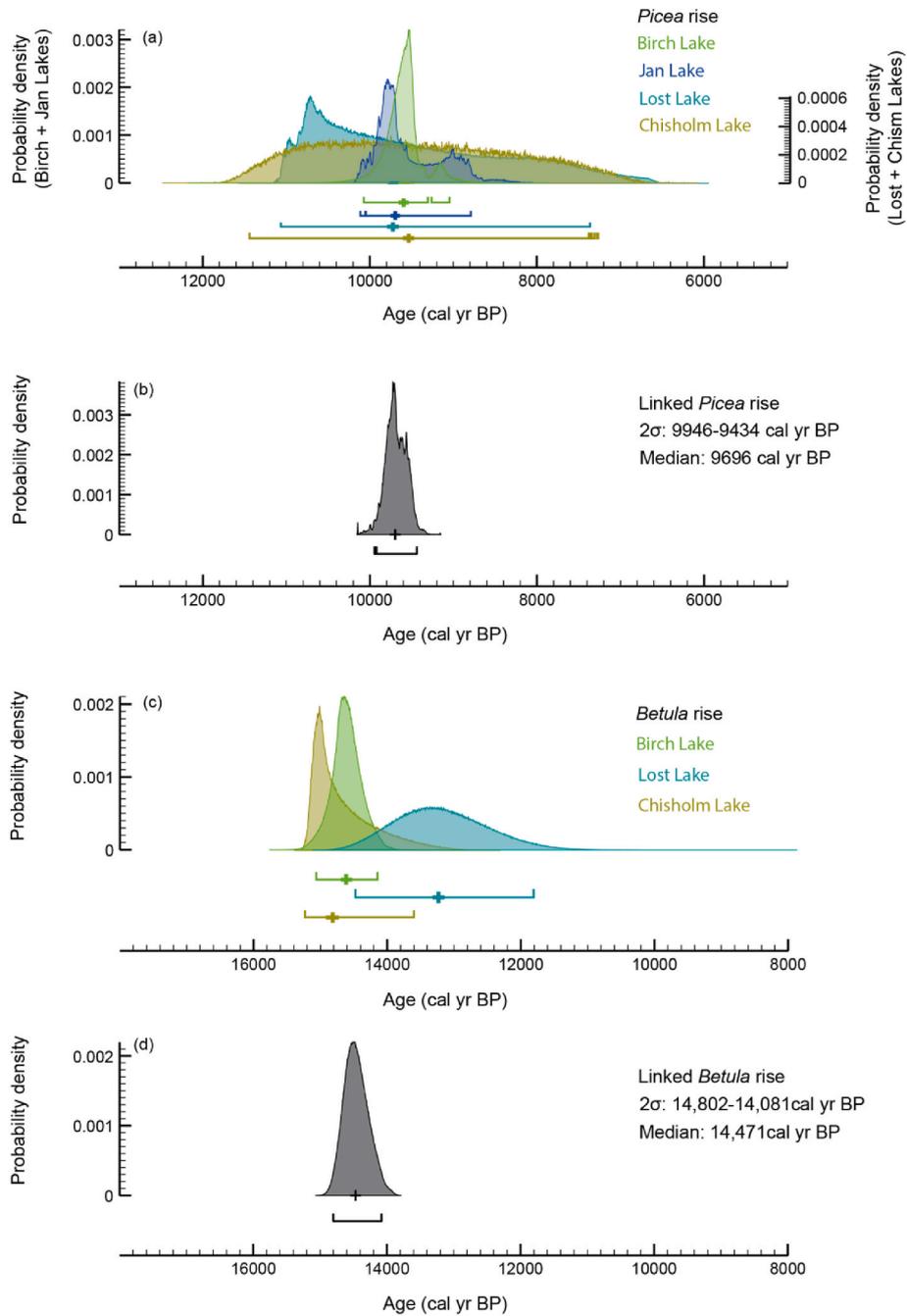
Fig. A1.2. Probability density functions for the four lakes used in the integrated age-depth model. Individual distributions in colour (a,c), linked distributions in grey (b,d).

Table A2
MAQ percent values for 120 samples (11 samples with zero repeats included)

Sample	Depth (cm)	Age (cal. yr BP)	MAQ score	Sample	Depth (cm)	Age (cal. yr BP)	MAQ score
Ala_CL-119	1	-109	0.988	Ala_CL-060	269	11015	0.900
Ala_CL-118	4	-7	1.000	Ala_CL-059	271	11113	0.950
Ala_CL-117	6	60	1.000	Ala_CL-058	274	11246	0.925
Ala_CL-116	11	229	0.625	Ala_CL-057	276	11324	0.850
Ala_CL-115	16	398	0.950	Ala_CL-056	279	11424	0.875
Ala_CL-114	21	567	1.000	Ala_CL-055	281	11480	0.963
Ala_CL-113	26	735	0.950	Ala_CL-054	284	11552	0.888
Ala_CL-112	31	904	0.950	Ala_CL-053	286	11597	1.000
Ala_CL-111	36	1073	0.963	Ala_CL-052	291	11697	0.825
Ala_CL-120	40	1151	1.000	Ala_CL-051	292	11720	1.000
Ala_CL-110	56		0.000	Ala_CL-050	296	11839	0.975
Ala_CL-109	61	1365	0.900	Ala_CL-049	301	12082	0.975
Ala_CL-108	66		0.000	Ala_CL-048	306	12346	1.000
Ala_CL-107	71	1445	0.988	Ala_CL-047	311	12502	0.950
Ala_CL-106	76		0.000	Ala_CL-046	316	12540	0.800
Ala_CL-105	81		0.000	Ala_CL-045	321	12563	0.800
Ala_CL-104	86		0.000	Ala_CL-044	326	12609	0.913
Ala_CL-103	91		0.000	Ala_CL-043	331	12689	0.975
Ala_CL-102	96		0.000	Ala_CL-042	336	12838	0.925
Ala_CL-101	101	2429	0.150	Ala_CL-041	341	13029	0.938
Ala_CL-100	106	2674	0.900	Ala_CL-040	346	13226	0.888
Ala_CL-099	111		0.000	Ala_CL-039	350	13387	0.100
Ala_CL-098	121	3424	1.000	Ala_CL-038	358	13713	0.988
Ala_CL-097	126		0.000	Ala_CL-037	363	13910	0.900
Ala_CL-096	131		0.000	Ala_CL-036	368	14094	0.863
Ala_CL-095	136	4170	0.888	Ala_CL-035	373	14246	0.800
Ala_CL-094	141		0.000	Ala_CL-034	378	14371	0.888
Ala_CL-093	145	4614	1.000	Ala_CL-033	383	14474	0.988
Ala_CL-092	155	5074	0.988	Ala_CL-032	388	14724	0.938
Ala_CL-091	158	5194	1.000	Ala_CL-031	393	15044	0.900
Ala_CL-090	160	5260	0.900	Ala_CL-030	397	15078	0.988
Ala_CL-089	165	5361	1.000	Ala_CL-029	399	15084	0.763
Ala_CL-088	170	5426	0.975	Ala_CL-028	401	15089	0.725
Ala_CL-087	175	5577	1.000	Ala_CL-027	403	15094	0.863
Ala_CL-086	180	5999	1.000	Ala_CL-026	405	15100	0.963
Ala_CL-085	185	6471	1.000	Ala_CL-025	408	15108	1.000
Ala_CL-084	190	6754	1.000	Ala_CL-024	409	15110	1.000
Ala_CL-083	195	6932	1.000	Ala_CL-023	411	15116	0.800
Ala_CL-082	200	7038	0.938	Ala_CL-022	413	15121	0.950
Ala_CL-081	205	7148	0.725	Ala_CL-021	415	15126	0.950
Ala_CL-080	210	7234	0.913	Ala_CL-020	417	15131	0.788
Ala_CL-079	215	7295	1.000	Ala_CL-019	419	15137	0.838
Ala_CL-078	218	7408	1.000	Ala_CL-018	421	15142	0.975
Ala_CL-077	220	7484	0.850	Ala_CL-017	423	15147	1.000
Ala_CL-076	225	8487	1.000	Ala_CL-016	425	15152	1.000
Ala_CL-075	228	9061	0.988	Ala_CL-015	427	15158	0.938
Ala_CL-074	230	9444	1.000	Ala_CL-014	429	15163	0.888
Ala_CL-073	233	9582	0.888	Ala_CL-013	431	15167	1.000
Ala_CL-072	235	9675	0.750	Ala_CL-012	433	15172	0.975
Ala_CL-071	238	9723	0.938	Ala_CL-011	435	15176	0.963
Ala_CL-070	240	9761	1.000	Ala_CL-010	437	15180	1.000
Ala_CL-069	242	9803	0.638	Ala_CL-009	439	15185	0.975
Ala_CL-068	246	9929	1.000	Ala_CL-008	441	15189	0.838
Ala_CL-067	249	10048	0.963	Ala_CL-007	443	15194	1.000
Ala_CL-066	251	10138	0.738	Ala_CL-006	445	15198	0.975
Ala_CL-065	254	10279	1.000	Ala_CL-005	447	15202	0.925
Ala_CL-064	259	10528	0.975	Ala_CL-004	449	15207	0.925
Ala_CL-063	261	10623	0.950	Ala_CL-003	451	15211	0.950
Ala_CL-062	264	10770	0.988	Ala_CL-002	453	15216	0.938
Ala_CL-061	266	10868	0.988	Ala_CL-001	455	15220	0.938

A3. All terrestrial plant *sed*aDNA records for Chisholm Lake.

Fig. A3a. Chisholm Lake, abundance of all trees, shrubs and graminoids shown as the proportion of PCR replicates (out of eight).

Fig. A3b. Chisholm Lake, forbs 1. Abundance of forbs shown as the proportion of PCR replicates (out of eight).
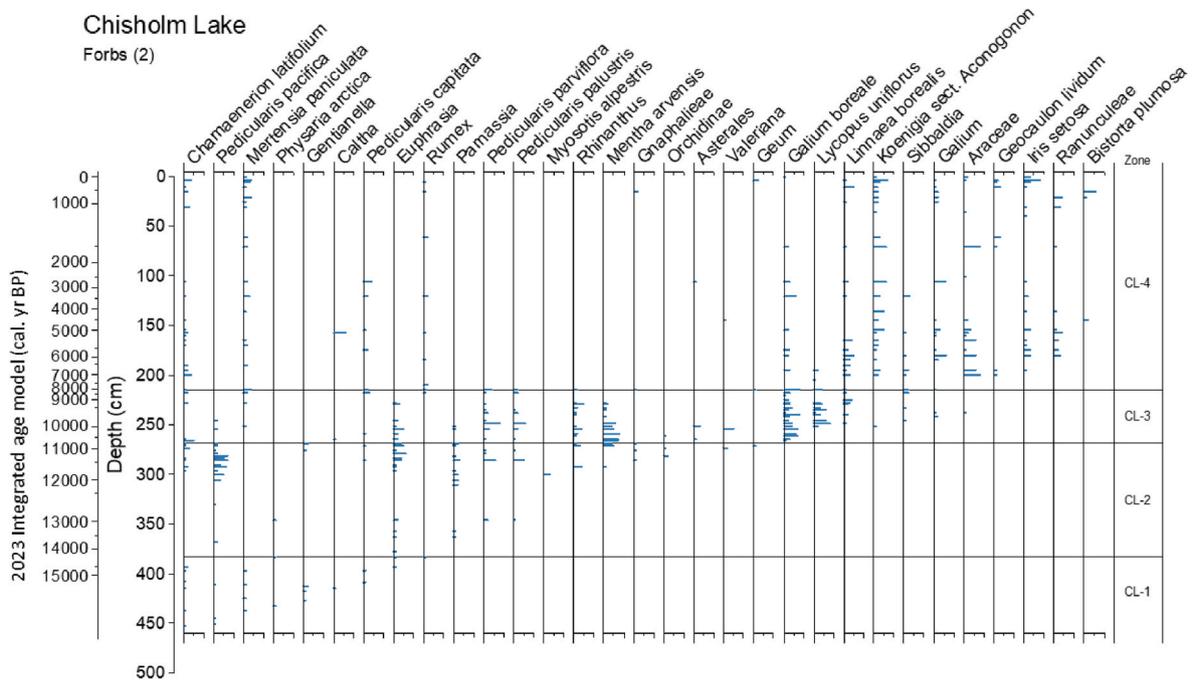
**Fig. A3c.** Chisholm Lake, forbs 2. Abundance of forbs shown as the proportion of PCR replicates (out of eight).
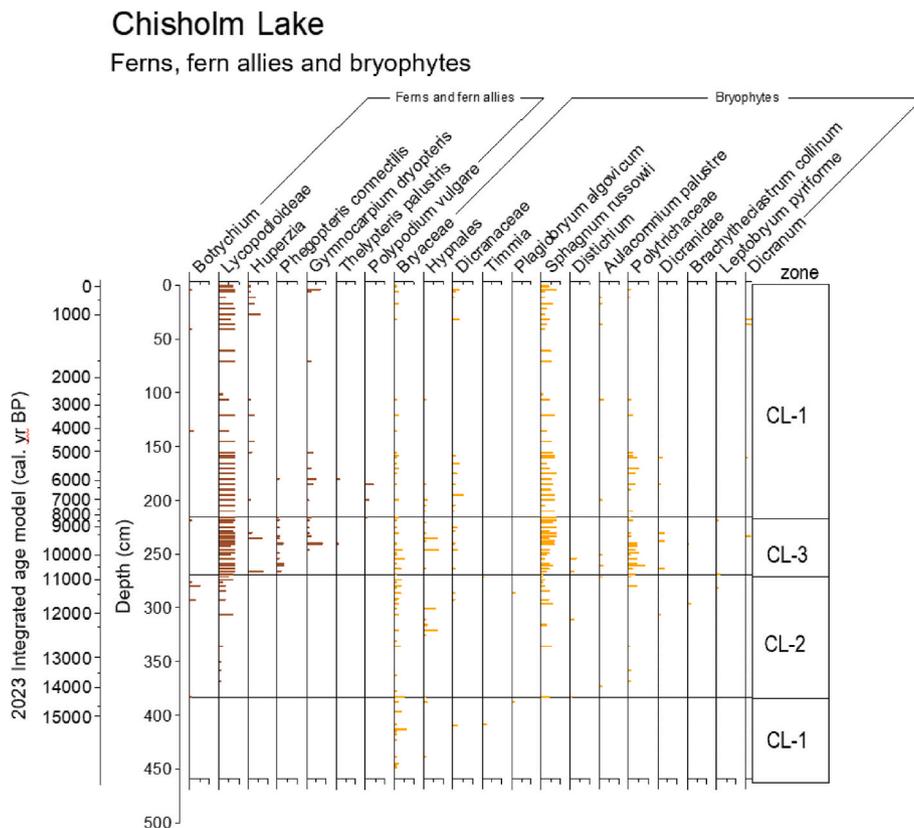
Fig. A3d. Chisholm Lake, abundance of ferns, fern allies, bryophytes shown by the proportion of PCR replicates (out of eight).

A 4. Taxon richness and turnover.

Chisholm Lake terrestrial taxon richness
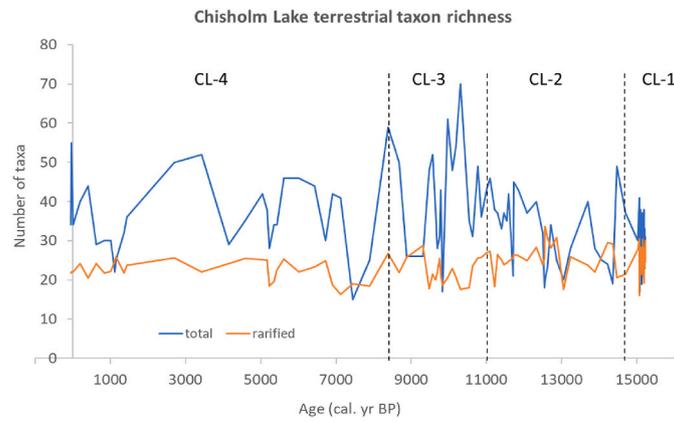
Fig. A4a. Total and rarefied richness for terrestrial plant taxa at Chisholm Lake. Zone boundaries defined by thin vertical lines.

Chisholm Lake aquatic taxon richness
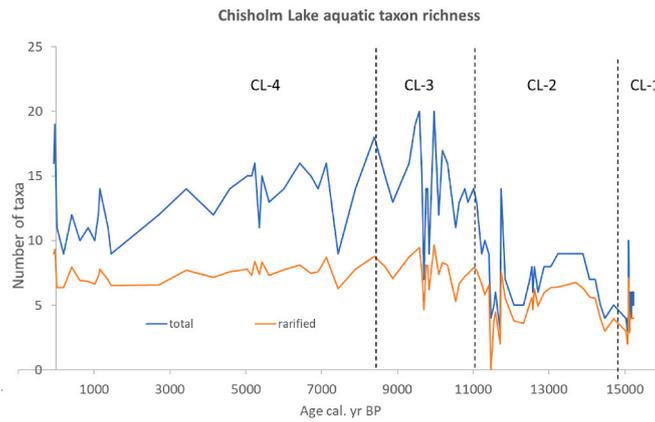
Fig. A4b. Rarefied and total richness for aquatic taxa plant at Chisholm Lake. Zone boundaries defined by thin vertical lines.

Chisholm Lake DCA Axis 1 scores (all taxa)
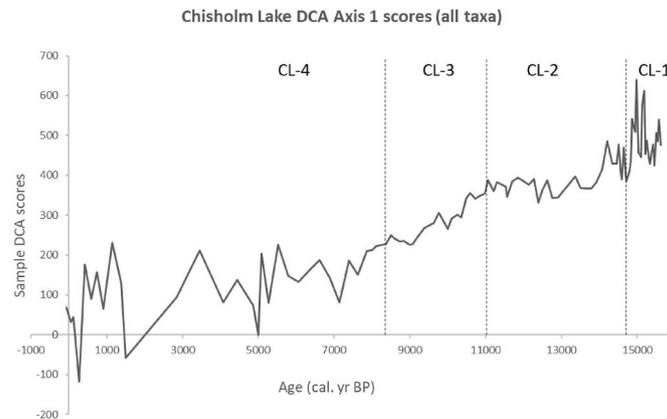
Fig. A4c. Scores for DCA axis one (all taxa, x-axis, 52.3% of total variation) over time (y-axis); the four *seda*DNA zones are defined by thin vertical lines.

A5. Topoclimates.

Chisholm Lake lies in a complex topographic setting between steep SW- and N-facing slopes (Fig. A5a). The SW slope would have continued below the current waterline when the level of Chisholm Lake was lower.
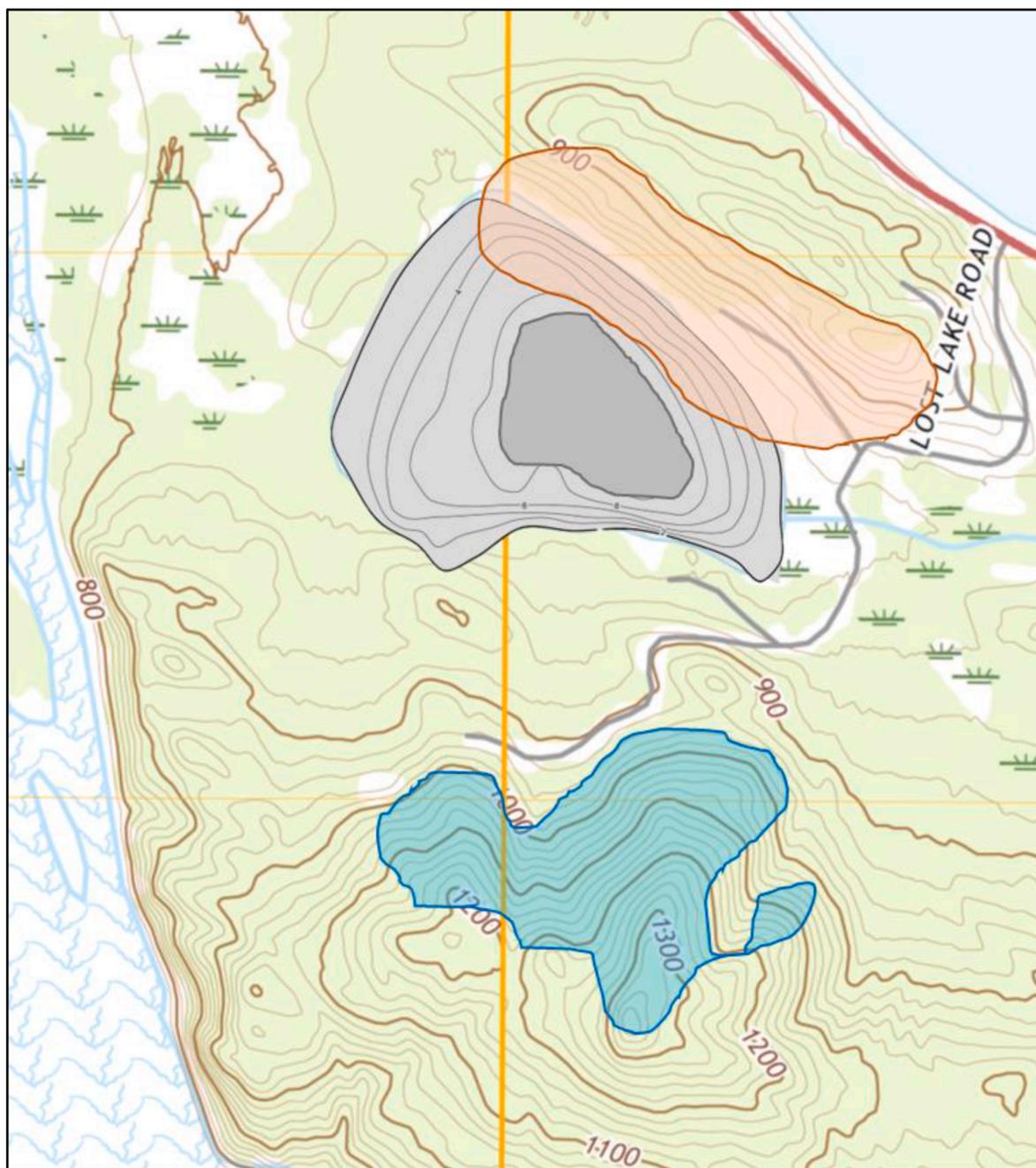
Fig. A5a. Part of Fig. 1 (main text) showing topography around Chisholm Lake. The red area denotes a steep SW-facing (warm) slope, the blue a steep N-facing (cold) slope. The lake (grey) shows contours above 8 m current depth, which is a conservative estimate of lake level during late-glacial aridity.

Elevational transects measured using Google Earth Pro across the SW-facing and N-facing slopes surrounding Chisholm Lake (Fig. A5b) have a maximum slope of ca. 20°. Using the equation of modern equivalent latitude (EL) of Lee (1964):

$$EL = \sin^{-1}(\sin \beta.\cos \alpha.\cos \lambda + \cos \beta.\sin \lambda) \tag{A1}$$

where α is azimuth from N, β is slope angle of inclination, and λ is latitude of the site, the equivalent latitude related to slope and aspect is estimated. The steepest measured angles were 21.8° for the SW-facing slope (A-B, ca. 220°) and 22.5° for the N-facing slope (C-D, ca. 355°, represented by an absolute deviation from N of 5°). Site latitude is 64.3° N. For ca. 20-degree slopes, the SW-facing slope EL is 45.5° and the N-facing EL is 86.2°. For less steep slopes of 10°, the EL values are 49.0° and 74.2°, respectively.
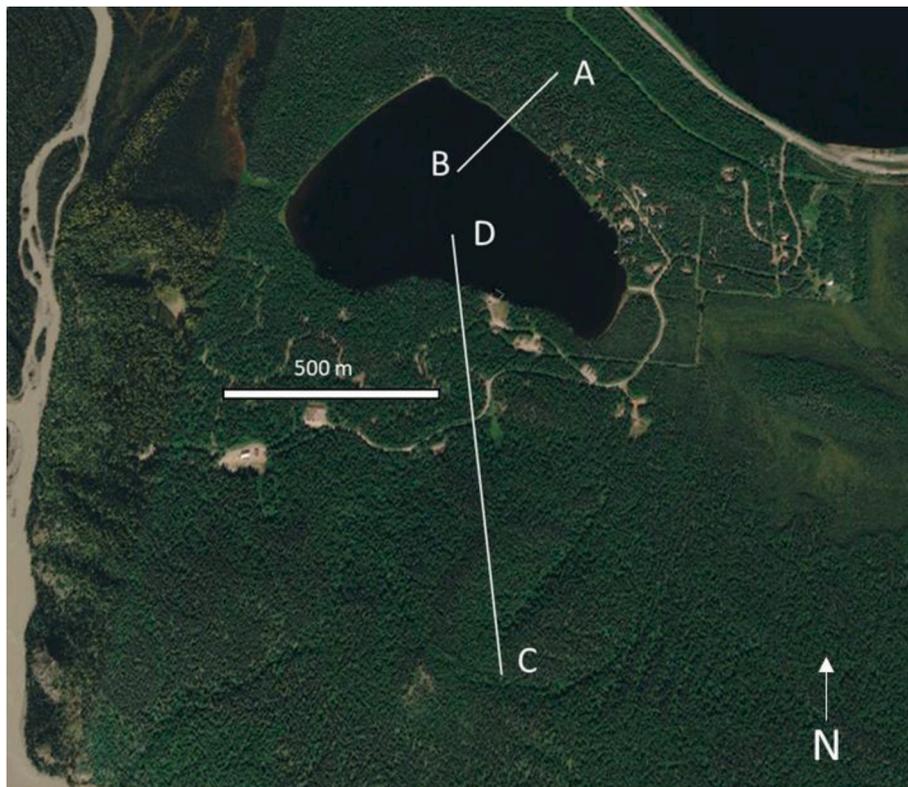
Fig. A5b. Location of two elevational transects at Chisholm Lake (image: Google Earth).

References

Abbott, R.J., Brochmann, C., 2003. History and evolution of the arctic flora: in the footsteps of Eric Hultén. Mol. Ecol. 12 (2), 299–313. https://doi.org/10.1046/j.1365-294X.2003.01731.x.

Abbott, M.B., Stafford, T.W., 1996. Radiocarbon geochemistry of modern and ancient arctic lake systems, Baffin Island, Canada. Quat. Res. 45 (3), 300–311. https://doi.org/10.1006/qres.1996.0031.

Abbott, M.B., Finney, B.P., Edwards, M.E., Kelts, K.R., 2000. Lake-level reconstruction and paleohydrology of birch Lake, central Alaska, based on seismic reflection profiles and core transects. Quat. Res. 53 (2), 154–166. https://doi.org/10.1006/qres.1999.2112.

Ager, T.A., 1975. *Late Quaternary Environmental History of the Tanana Valley, Alaska.* Ph. D. Thesis. Ohio State University, Ohio, p. 184.

Alaska Department of Fish and Game , https://www.adfg.alaska.gov/SF_Lakes. Accessed 23/March/2023.

Alsos, I.G., Sjögren, P., Edwards, M.E., Landvik, J.Y., Gielly, L., Forwick, M., Coissac, E., Brown, A.G., Jakobsen, L.V., Føreid, M.K., Pedersen, M.W., 2016. Sedimentary ancient DNA from Lake Skartjørna, Svalbard: assessing the resilience of arctic flora to Holocene climate change. Holocene 26 (4), 627–642. https://doi.org/10.1177/0959683615612563.

Alsos, I.G., Lammers, Y., Yoccoz, N.G., Jørgensen, T., Sjögren, P., Gielly, L., Edwards, M. E., 2018. Plant DNA metabarcoding of lake sediments: how does it represent the contemporary vegetation? PLoS One 13 (4), e0195403. https://doi.org/10.1371/journal.pone.0195403.

Alsos, I.G., Sjögren, P., Brown, A.G., Gielly, L., Merkel, M.K.F., Paus, A., Lammers, Y., Edwards, M.E., Alm, T., Leng, M., Goslar, T., Langdon, C.T., Bakke, J., van der Bilt, W.G.M., 2020. Last Glacial Maximum environmental conditions at Andøya, northern Norway; evidence for a northern ice-edge ecological "hotspot". Quat. Sci. Rev. 239, 106364 https://doi.org/10.1016/j.quascirev.2020.106364.

Alsos, I.G., Lammers, Y., Kjellman, S.E., Merkel, M.F., Bender, E.M., Rouillard, A., Erlendson, E., Guðmundsdóttir, E.R., Bendiktsson, Í.Ö., Farnsworth, W.R., Brynjólfsson, S., Gísladóttir, G., Eddudóttir Schomacker, A., 2021. Ancient sedimentary DNA shows rapid post-glacial colonisation of Iceland followed by relatively stable vegetation until the Norse settlement (Landnám) AD 870. Quat. Sci. Rev. 259, 106903 https://doi.org/10.1016/j.quascirev.2021.106903.

Anderson, P.M., Bartlein, P.J., Brubaker, L.B., Gajewski, K., Ritchie, J.C., 1989. Modern analogues of late-Quaternary pollen spectra from the western interior of North America. J. Biogeogr. 16, 573–596. https://doi.org/10.2307/2845212.

Anderson, P.M., Edwards, M.E., Brubaker, L.B., 2004. Results and paleoclimate implications of 35 years of paleoecological research in Alaska. Dev. Quat. Sci. 1, 427–440.

Anderson, L.L., Hu, F.S., Nelson, D.M., Petit, R.J., Paige, K.N., 2006. Ice-age endurance: DNA evidence of a white spruce refugium in Alaska. Proc. Natl. Acad. Sci. USA 103, 12447–12450. https://doi.org/10.1073/pnas.0605310103.

Anderson, L.L., Hu, F.S., Paige, K.N., 2011. Phylogeographic history of white spruce during the last glacial maximum: uncovering cryptic refugia. J. Hered. 102, 207–216. https://doi.org/10.1093/jhered/esq110.

Bakker, E.S., Gill, J.L., Johnson, C.N., Vera, F.W., Sandom, C.J., Asner, G.P., Svenning, J. C., 2016. Combining paleo-data and modern exclosure experiments to assess the impact of megafauna extinctions on woody vegetation. Proc. Natl. Acad. Sci. USA 113, 847–855. https://doi.org/10.1073/pnas.1502545112.

Barber, V.A., Finney, B.P., 2000. Late Quaternary paleoclimatic reconstructions for interior Alaska based on paleolake-level data and hydrologic models. J. Paleolimnol. 24, 29–41. https://doi.org/10.1016/S1571-0866(03)01019-4.

Bartlein, P.J., Anderson, P.M., Edwards, M.E., McDowell, P.F., 1991. A framework for interpreting paleoclimatic variations in eastern Beringia. Quat. Int. 10–12, 73–83. https://doi.org/10.1016/1040-6182(91)90041-L.

Bartlein, P.J., Hostetler, S.W., Alder, J.R., 2014. Paleoclimate. In: Ohring, G. (Ed.), Climate Change in North America, Regional Climate Studies. Springer, New York, pp. 1–51. https://doi.org/10.1007/978-3-319-03768-4_1.

Bartlein, P.J., Edwards, M.E., Hostetler, S.W., Shafer, S.L., Anderson, P.M., Brubaker, L. B., Lozhkin, A.V., 2015. Early-Holocene warming in Beringia and its mediation by sea-level and vegetation changes. Clim. Past 11, 1197–1222. https://doi.org/10.5194/cp-11-1197-2015.

Bennett, K.D., Parducci, L., 2006. DNA from pollen: principles and potential. Holocene 16, 1031–1034. https://doi.org/10.1177/0959683606069383.

Berger, A., Loutre, M.F., 1991. Insolation values for the climate of the last 10 million years. Quat. Sci. Rev. 10, 297–317. https://doi.org/10.1016/0277-3791(91)90033-Q.

Bigelow, N.H., 1997. Late Quaternary Vegetation and Lake Level Changes in Central Alaska. University of Alaska Fairbanks. PhD Thesis.

Bigelow, N.H., Edwards, M.E., 2001. A 14,000 yr paleoenvironmental record from windmill lake, central Alaska: lateglacial and Holocene vegetation in the Alaska range. Quat. Sci. Rev. 20 (1–3), 203–215. https://doi.org/10.1016/S0277-3791(00)00122-0.

Boyer, F., Mercier, C., Bonin, A., Le Bras, Y., Taberlet, P., Coissac, E., 2016. ObiTools: a UNIX-inspired software package for DNA metabarcoding. Mol. Ecol. Res. 16, 176–182. https://doi.org/10.1111/1755-0998.12428.

Briner, J.P., Tulenko, J.P., Kaufman, D.S., Young, N.E., Baichtal, J.F., Lesner, A., 2017. The last deglaciation of Alaska. Geogr. Res. Lett. 43, 429–448. https://doi.org/10.18172/cig.3229.

Bronk Ramsey, C., 2008. Deposition models for chronological records. Quat. Sci. Rev. 27 (1–2), 42–60. https://doi.org/10.1016/j.quascirev.2007.01.019.

Bronk Ramsey, C., 2009. Bayesian analysis of radiocarbon dates. Radiocarbon 51 (1), 337–360.

Bronk Ramsey, C., 2009a. Bayesian analysis of radiocarbon dates. Radiocarbon 51 (1), 337–360. https://doi.org/10.1017/S0033822200033865.

Bronk Ramsey, C., 2009b. Dealing with outliers and offsets in radiocarbon dating. Radiocarbon 51 (3), 1023–1045. https://doi.org/10.1017/S0033822200034093.

Bronk Ramsey, C., Lee, S., 2013. Recent and planned developments of the program OxCal. Radiocarbon 55 (2), 720–730. https://doi.org/10.1017/S0033822200057878.

Brubaker, L.B., Anderson, P.M., Edwards, M.E., Lozhkin, A.V., 2005. Beringia as a glacial refugium for boreal trees and shrubs: new perspectives from mapped pollen data. J. Biogeogr. 32 (5), 833–848. https://doi.org/10.1111/j.1365-2699.2004.01203.x.

Carlson, L.J., Finney, B., 2004. A 13 000-year history of vegetation and environmental change at Jan Lake, east-central Alaska. Holocene 14 (6), 818–827. https://doi.org/10.1191/0959683604hl762rp.

Chytrý, M., Horsák, M., Danihelka, J., Ermakov, N., German, D.A., Hájek, M., Hájková, P., Kočí, M., Kubešová, S., Lustyk, P., Nekola, J.C., 2019. A modern analogue of the Pleistocene steppe-tundra ecosystem in southern Siberia. Boreas 48, 36–56. https://doi.org/10.1111/bor.12338.

Clark, P.U., Dyke, A.S., Shakun, J.D., Carlson, A.E., Clark, J., Wohlfarth, B., Mitrovica, J. X., Hostetler, S.W., McCabe, A.M., 2009. The last glacial maximum. Science 325 (5941), 710–714. https://doi.org/10.1126/science.1172873.

Clarke, C.L., Edwards, M.E., Gielly, L., Ehrich, D., Hughes, P.D.M., Morozova, L.M., Haflidason, H., Mangerud, J., Svendsen, J.I., Alsos, I.G., 2019. Persistence of arctic-alpine flora during 24,000 years of environmental change in the Polar Urals. Sci. Rep. 9, 19613 https://doi.org/10.1038/s41598-019-55989-9.

Clarke, C.L., Alsos, I.G., Edwards, M.E., Paus, A., Gielly, L., Haflidason, H., Mangerud, J., Regnéll, C., Hughes, P.D.M., Svendsen, J.I., Bjune, A.E., 2020. A 24,000-year ancient DNA and pollen record from the Polar Urals reveals temporal dynamics of arctic and boreal plant communities. Quat. Sci. Rev. 247, 106564 https://doi.org/10.1016/j.quascirev.2020.106564.

Colinvaux, P.A., 1964. The environment of the bering land bridge. Ecol. Monogr. 34, 297–329. https://doi.org/10.2307/1948504.

Coulter, H.W., Hopkins, D.M., Karlstrom, T.N.V., Péwé, T.L., Wahrhaftig, C., Williams, J. R., 1965. Map Showing Extent of Glaciations in Alaska, vols. I-415. U.S. Geological Survey Map. https://doi.org/10.3133/i415.

Cwynar, L.C., 1982. A late quaternary vegetation history from Hanging lake, northern Yukon. Ecol. Monogr. 52 (1), 1–24. https://doi.org/10.2307/2937342.

Cwynar, L.C., Ritchie, J.C., 1980. Arctic steppe-tundra: a Yukon perspective. Science 20, 1375–1377. https://doi.org/10.1126/science.208.4450.1375.

Dyke, A.S., Andrews, J.T., Clark, P.U., Miller, G.H., Shaw, J., Veillette, J.J., 2002. The Laurentide and innuitian ice sheets during the last glacial maximum. Quat. Sci. Rev. 21 (1–3), 9–31. https://doi.org/10.1016/S0277-3791(01)00095-6.

Edwards, M.E., Armbruster, W.S., 1989. A tundra-steppe transition on Kathul Mountain, Alaska, USA. Arctic Antarct. Alpine Res. 21, 296–304. https://doi.org/10.1080/00040851.1989.12002742.

Edwards, M.E., Bigelow, N.H., Finney, B.P., Eisner, W.R., 2000. Records of aquatic pollen and sediment properties as indicators of late-Quaternary Alaskan lake levels. J. Paleolimnol. 24 (1), 55–68. https://doi.org/10.1023/A:1008117816612.

Edwards, M.E., Brubaker, L.B., Anderson, P.M., Lozhkin, A.V., 2005. Structurally novel biomes: a response to past warming in Beringia. Ecology 86, 1696–1703. https://doi.org/10.1890/03-0787.

Edwards, M.E., Armbruster, W.S., Elias, S.A., 2014. Constraints on post-glacial boreal tree expansion out of far-northern refugia. Global Ecol. Biogeogr. 23 (11), 1198–1208. https://doi.org/10.1111/geb.12213.

Edwards, M.E., Lloyd, A., Armbruster, W.S., 2018. Assembly of Alaska-Yukon boreal steppe communities: testing biogeographic hypotheses via modern ecological distributions. J. Systemat. Evol. 56, 466–475. https://doi.org/10.1111/jse.12307.

Ficetola, G.F., Coissac, E., Zundel, S., Riaz, T., Shehzad, W., Bessiere, J., Taberlet, P., Pompagnin, F., 2010. An in silico approach for the evaluation of DNA barcodes. BMC Genom. 11, 434. https://doi.org/10.1186/1471-2164-11-434, 2010.

Finkenbinder, M.S., Abbott, M.B., Edwards, M.E., Langdon, C.T., Steinman, B.A., Finney, B.P., 2014. A 31,000 year record of paleoenvironmental and lake-level change from Harding Lake, Alaska, USA. Quat. Sci. Rev. 87, 98–113. https://doi.org/10.1016/j.quascirev.2014.01.005.

Giguet-Covex, C., Ficetola, G.F., Walsh, K., Poulenard, J., Bajard, M., Fouinat, L., Sabatier, P., Gielly, L., Messager, E., Develle, A.L., David, F., Taberlet, P., Brisset, E., Guiter, F., Sinet, R., Arnaud, F., 2019. New insights on lake sediment DNA from the catchment: importance of taphonomic and analytical issues on the record quality. Sci. Rep. 9, 14676 https://doi.org/10.1038/s41598-019-50339-1, 2019.

Giguet-Covex, C., Jelavić, S., Foucher, A., Morlock, M.A., Wood, S.A., Augustijns, F., Domaizon, I., Gielly, L., Capo, E., 2023. The sources and fates of lake sedimentary DNA. In: Capo, E., Barouillet, C., Smol, J.P. (Eds.), Tracking Environmental Change Using Lake Sediments, Developments in Paleoenvironmental Research, vol. 21. Springer, Cham. https://doi.org/10.1007/978-3-031-43799-1_2.

Goetcheus, V.G., Birks, H.H., 2001. Full-glacial upland tundra vegetation preserved under tephra in the Beringia National Park, Seward Peninsula, Alaska. Quat. Sci. Rev. 20, 135–147. https://doi.org/10.1016/S0277-3791(00)00127-X.

Graham, R.W., Belmecheri, S., Choy, K., Culleton, B.J., Davies, L.J., Froese, D., Heintzman, P.D., Hritz, C., Knapp, J.D., Newsom, L.A., Rawcliffe, R., Saulnier-Talbot, E., Shapiro, B., Wang, Y., Williams, J.W., 2016. Timing and causes of mid-Holocene mammoth extinction on St. Paul Island, Alaska. Proc. Natl. Acad. Sci. USA 113, 9310–9314. https://doi.org/10.1073/pnas.1604903113.

Grimm, E.C., 1987. CONISS: a FORTRAN 77 program for stratigraphically constrained cluster analysis by the method of incremental sum of squares. Comput. Geosci. 13, 13–37. https://doi.org/10.1016/0098-3004(87)90022-7.

Grimm, E.C., 1992. Tilia and Tilia-graph: pollen spreadsheet and graphics programs. Programs and Abstracts, 8th International Palynological Congress, Aix-en-Provence 56. September 6-12, 1992.

Guthrie, R.D., 1982. Mammals of the mammoth steppe as paleoenvironmental indicators. In: Hopkins, D.M., Matthews, J.V., Schweger, C.E., Young, S.B. (Eds.), Palaeoecology of Beringia. Academic Press, pp. 307–326. https://doi.org/10.1016/B978-0-12-355860-2.50030-2.

Guthrie, R.D., 1990. Frozen Fauna of the Mammoth Steppe: the Story of Blue Babe. University of Chicago Press, Chicago.

Guthrie, R.D., 2006. New carbon dates link climatic change with human colonization and Pleistocene extinctions. Nature 441, 207–209. https://doi.org/10.1038/nature04604.

Hammer, Ø., Harper, D.A.T., Ryan, P.D., 2001. PAST: paleontological statistics software package for education and data analysis. Palaeontol. Electron. 4 (1), 9.

Heiri, O., Lotter, A.F., Lemcke, G., 2001. Loss on ignition as a method for estimating organic and carbonate content in sediments: reproducibility and comparability of results. J. Paleolimnol. 25, 101–110. https://doi.org/10.1023/A:1008119611481.

Holmes, C.E., 2001. Between two worlds: late Pleistocene cultural and technological diversity in eastern Beringia. Arctic Anthropol. 38, 154–170.

Holmes, C.E., 2008. The taiga period: Holocene archaeology of the northern boreal forest, Alaska: Alaska J. Anthropol. 6, 69–81.

Hopkins, D.M., 1982. Aspects of the paleogeography of Beringia during the late Pleistocene. In: Hopkins, D.M., Matthews Jr, J.V., Schweger, C.E., Young, S.B. (Eds.), Paleoecology of Beringia. Academic Press, New York, pp. 3–28.

Hopkins, D.M., Smith, P.A., Matthews, J.V., 1981. Dated wood from Alaska and the Yukon: implications for forest refugia in Beringia. Quat. Res. 15 (3), 217–249. https://doi.org/10.1016/0033-5894(81)90028-4.

Hopkins, D.M., Matthews, J.V., Schweger, C.E., Young, S.B. (Eds.), 1982. Paleoecology of Beringia. Academic Press, New York, p. 504.

Hughes, A.L.C., Gyllencreutz, R., Lohne, Ø.S., Mangerud, J., Svendsen, J.I., 2016. The last Eurasian ice sheets- a chronological database and time-slice reconstruction, DATED-1. Boreas 45 (1), 1–45. https://doi.org/10.1111/bor.12142.

Hultén, E., 1937. Outline of the history of arctic and boreal biota during the Quaternary period: Stockholm. Thule 168.

Hultén, E., 1968. Flora of Alaska and Neighboring Territories. Stanford. Stanford University Press, pp. 1032–pp.

Jones, M.C., Yu, Z., 2010. Rapid deglacial and early Holocene expansion of peatlands in Alaska. Proc. Natl. Acad. Sci. U.S.A. 107, 7347–7352.

Jørgensen, T., Haile, J., Möller, P., Andreev, A., Boessenkool, S., Rasmussen, M., Kienast, F., Coissac, E., Taberlet, P., Brochmann, C., Bigelow, N.H., Andersen, K., Orlando, L., Gilbert, M.T.P., Willerslev, E., 2012. A comparative study of ancient sedimentary DNA, pollen and macrofossils from permafrost sediments of northern Siberia reveals long-term vegetational stability. Mol. Ecol 21, 1989–2003. https://doi.org/10.1111/j.1365-294X.2011.05287.x.

Jorgenson, M.T., Yoshikawa, K., Kanveskiy, M., Shur, Y., Romanovsky, V., Marchenko, S., Grosse, G., Brown, J., Jones, B., 2008. Permafrost characteristics of Alaska. Proceedings of the Ninth International Conference on Permafrost 3, 121–122.

Kaufman, D.S., Manley, W.F., 2004. Pleistocene maximum and late wisconsinan glacier extents across Alaska, USA. Dev. Quat. Sci. 2 (Part B), 9–27. https://doi.org/10.1016/S1571-0866(04)80182-9.

Kaufman, D.S., Ager, T.A., Anderson, N.J., Anderson, P.M., Andrews, J.T., Bartlein, P.J., Brubaker, L.B., Coats, L.L., Cwynar, L.C., Duvall, M.L., Dyke, A.S., Edwards, M.E., Eisner, W.R., Gajewski, K., Geirsdottir, A., Hu, F.S., Jennings, A.E., Kaplan, M.R., Kerwin, M.W., Lozhkin, A.V., MacDonald, G.M., Miller, G.H., Mock, C.J., Oswald, W. W., Otto-Bliesner, B.L., Porinchu, D.F., Ruhland, K., Smol, J.P., Steig, E.J., Wolfe, B. B., 2004. Holocene thermal maximum in the western Arctic (0–180° W). Quat. Sci. Rev. 23, 529–560. https://doi.org/10.1016/j.quascirev.2003.09.007.

Kielhofer, J., Miller, C., Reuther, J., Holmes, C., Potter, B., Lanoë, F.B., Crass, B., 2020. The micromorphology of loess-paleosol sequences in central Alaska: a new perspective on soil formation and landscape evolution since the Late Glacial period (c. 16,000 cal yr BP to present). Geoarchaeology 35 (5), 701–728. https://doi.org/10.1002/gea.21807.

Kielhofer, J.R., Tierney, J.E., Reuther, J.D., Potter, B., Holmes, C.E., Lanoë, F., Esdale, J., Wooller, M., Bigelow, N., 2022. BrGDGT-based temperature reconstructions in loess from Central Alaska: opportunities, challenges, and limitations in an arid, high latitude environment. Quat. Sci. Rev. 303, 107979 https://doi.org/10.1016/j.quascirev.2023.107979.

Kienast, F., Siegert, C., Dereviagin, A., Mai, D.H., 2001. Climatic implications of late quaternary plant macrofossil assemblages from the taymyr Peninsula, Siberia. Global Planet. Change 31 (1–4), 265–281. https://doi.org/10.1016/S0921-8181(01)00124-2.

Kienast, F., Schirrmeister, L., Siegert, C., Tarasov, P., 2005. Palaeobotanical evidence for warm summers in the East Siberian Arctic during the last cold stage. Quat. Res. 63, 283–300. https://doi.org/10.1016/j.yqres.2005.01.003.

Kraaijeveld, K., de Weger, L.A., García, M.V., Buermans, H., Frank, J., Hiemstra, P.S., den Dunnen, J.T., 2015. Efficient and sensitive identification and quantification of airborne pollen using next-generation DNA sequencing. Mol. Ecol. Res. 15, 8–16. https://doi.org/10.1111/1755-0998.12288.

Lee, R., 1964. Potential insolation as a topoclimatic characterstic of drainiage basins. Int. Assoc. Sci. Hydrol. 9, 27–41. https://doi.org/10.1080/02626666409493652.

Lloyd, A.H., Armbruster, W.S., Edwards, M.E., 1994. Ecology of a steppe-tundra gradient in interior Alaska. J. Veg. Sci. 5, 897–912. https://doi.org/10.2307/3236202.

Lora, J.M., Mitchell, J.L., Tripati, A.E., 2016. Abrupt reorganization of North Pacific and western North American climate during the last deglaciation. Geophys. Res. Lett. 43, 11–796. https://doi.org/10.1002/2016GL071244.

Lynch, J.A., Hollis, J.A., Hu, F.S., 2004. Climatic and landscape controls of the boreal forest fire regime: Holocene records from Alaska. J. Ecol. 92, 477–489. https://doi.org/10.1111/j.0022-0477.2004.00879.x.

Mann, D.H., Peteet, D.M., Reanier, R.E., Kunz, M.L., 2002. Responses of an arctic landscape to Lateglacial and early Holocene climatic changes: the importance of moisture. Quat. Sci. Rev. 21, 997–1021. https://doi.org/10.1016/S0277-3791(01)00116-0.

Mann, D.H., Groves, P., Kunz, M.L., Reanier, R.E., Gaglioti, B.V., 2013. Ice-age megafauna in Arctic Alaska: extinction, invasion, survival. Quat. Sci. Rev. 70, 91–108. https://doi.org/10.1016/j.quascirev.2013.03.015.

Mann, D.H., Groves, P., Gaglioti, B.V., Shapiro, B., 2019. Climate-driven ecological stability as a globally shared cause of Late Quaternary megafaunal extinctions: the Plaids and Stripes Hypothesis. Biol. Rev. 94, 328–352. https://doi.org/10.1111/brv.12456.

Monteath, A.J., Gaglioti, B.V., Edwards, M.E., Froese, D., 2021. Late Pleistocene shrub expansion preceded megafauna turnover and extinctions in eastern Beringia. Proc. Natl. Acad. Sci. USA 118 (52), e2107977118. https://doi.org/10.1073/pnas.2107977118.

Monteath, A.J., Kuzmina, S., Mahony, M., Calmels, F., Porter, T., Mathewes, R., Sanborn, P., Zazula, G., Shapiro, B., Murchie, T.J., Poinar, H.N., 2023. Relict permafrost preserves megafauna, insects, pollen, soils and pore-ice isotopes of the mammoth steppe and its collapse in central Yukon. Quat. Sci. Rev. 299, 107878 https://doi.org/10.1016/j.quascirev.2022.107878.

Muhs, D.R., Ager, T.A., Bettis III, E.A., McGeehin, J., Been, J.M., Begét, J.E., Pavich, M.J., Stafford Jr, T.W., De Anne, S.P., 2003. Stratigraphy and palaeoclimatic significance of Late Quaternary loess–palaeosol sequences of the Last Interglacial–Glacial cycle in central Alaska. Quat. Sci. Rev. 22, 1947–1986. https://doi.org/10.1016/S0277-3791(03)00167-7.

Murchie, T.J., Monteath, A.J., Mahony, M.E., Long, G.S., Cocker, S., Sadoway, T., Karpinski, E., Zazula, G., MacPhee, R.D., Froese, D., Poinar, H.N., 2021a. Collapse of the mammoth-steppe in central Yukon as revealed by ancient environmental DNA. Nat. Commun. 12 (1), 7120. https://doi.org/10.1038/s41467-021-27439-6.

Murchie, T.J., Kuch, M., Duggan, A.T., Ledger, M.L., Roche, K., Klunk, J., Karpinski, E., Hackenberger, D., Sadoway, T., MacPhee, R., Froese, D., 2021b. Optimizing extraction and targeted capture of ancient environmental DNA for reconstructing past environments using the PalaeoChip Arctic-1.0 bait-set. Quat. Res. 99, 305–328. https://doi.org/10.1017/qua.2020.59.

Murray, D.F., Murray, B.M., Yurtsev, B.A., Howenstein, R., 1983. Biogeographic significance of steppe vegetation in subarctic Alaska. In: Proceedings of the IV International Permafrost Conference, Fairbanks. National Academy Press, Washington, D.C., pp. 883–888

Myers-Smith, I.H., Forbes, B.C., Wilmking, M., Hallinger, M., Lantz, T., Blok, D., Tape, K. D., Macias-Fauria, M., Sass-Klaassen, U., Lévesque, E., Boudreau, S., et al., 2011. Shrub expansion in tundra ecosystems: dynamics, impacts and research priorities. Environ. Res. Lett. 6, 045509 https://doi.org/10.1088/1748-9326/6/4/045509.

Nakao, K., Ager, T.A., 1985. Climatic changes and vegetational history of the interior of Alaska inferred from drilled cores at Harding Lake. In: Nakao, K. (Ed.), Hydrological Regime and Climatic Changes in the Arctic Circle. Report of the Alaskan Paleohydrology Research Project, Laboratory of Hydrology, Department of Geophysics. Faculty of Science. Hokkaido University, Japan.

Nichols, R.V., Vollmers, C., Newsom, L.A., Heintzman, P.D., Leighton, M., Green, R.E., Shapiro, B., 2018. Minimizing polymerase biases in metabarcoding. Mol. Ecol. Res. 18, 927–939. https://doi.org/10.1111/1755-0998.12895.

Olofsson, J., Oksanen, L., Callaghan, T., Hulme, P.E., Oksanen, T., Suominen, O., 2009. Herbivores inhibit climate-driven shrub expansion on the tundra. Global Change Biol. 15, 2681–2693. https://doi.org/10.1111/j.1365-2486.2009.01935.x.

Parducci, L., Edwards, M.E., Bennett, K.D., Alm, T., Elverland, E., Tollefsrud, M.M., Jørgensen, T., Houmark-Nielsen, M., Larsen, N.K., Kjær, K.H., Fontana, S.L., Alsos, I. G., Willerslev, E., 2012a. Response to comment on "glacial survival of boreal trees in northern scandinavia". Science 338, 742. https://doi.org/10.1126/science.1225476.

Parducci, L., Jørgensen, T., Tollefsrud, M.M., Elverland, E., Alm, T., Fontana, S.L., Bennett, K.D., Haile, J., Matetovici, I., Suyama, Y., Edwards, M.E., Andersen, K., Rasmussen, M., Boessenkool, S., Coissac, E., Brochmann, C., Taberlet, P., Houmark-Nielsen, M., Larsen, N.K., Orlando, L., Gilbert, M.T.P., Kjær, K.H., Alsos, I.G., Willerslev, E., 2012b. Glacial survival of boreal trees in northern Scandinavia. Science 335, 1083–1086. https://doi.org/10.1126/science.1216043.

Parducci, L., Bennett, K.D., Ficetola, G.F., Alsos, I.G., Suyama, Y., Wood, J.R., Pedersen, M.W., 2017. Ancient plant DNA in lake sediments. New Phytol. 214, 924–942. https://doi.org/10.1111/nph.14470.

Pedersen, M.W., Ruter, A., Schweger, C., Friebe, H., Staff, R.A., Kjeldsen, K.K., Mendoza, M.L.Z., Beaudoin, A.B., Zutter, C., Larsen, N.K., Potter, B.A., Nielsen, R., Rainville, R.A., Orlando, L., Meltzer, D.J., Kjær, K.H., Willerslev, E., 2016. Postglacial viability and colonization in North America's ice-free corridor. Nature 537, 45–59. https://doi.org/10.1038/nature19085.

Péwé, T.L., 1975. Quaternary Geology of Alaska 835. US Government Printing Office.

Potter, B.A., 2008. Radiocarbon chronology of central Alaska: technological continuity and economic change. Radiocarbon 50 (2), 181–204. https://doi.org/10.1017/S0033822200033518.

Potter, B.A., Halffman, C.M., McKinney, H.J., Reuther, J.D., Finney, B.P., Lanoë, F.B., López, J.A., Holmes, C.E., Palmer, E., Capps, M., Kemp, B.M., 2023. Freshwater and anadromous fishing in Ice Age Beringia. Sci 9, eadg6802.

Potter, B.A., Irish, J.D., Reuther, J.D., Gelvin-Reymiller, C., Holliday, V.T., 2011. A terminal Pleistocene child cremation and residential structure from eastern Beringia. Science 331 (6020), 1058–1062. https://doi.org/10.1126/science.1201581.

Potter, B.A., Irish, J.D., Reuther, J.D., McKinney, H.J., 2014. New insights into Eastern Beringian mortuary behavior: a terminal Pleistocene double infant burial at Upward Sun River. Proc. Natl. Acad. Sci. USA 48, 17060–17065. https://doi.org/10.1073/pnas.1413131111.

Potter, B.A., Reuther, J.D., Holliday, V.T., Holmes, C.E., Miller, D.S., Schmuck, N., 2017. Early colonization of Beringia and northern NorthNorth America: chronology, routes, and adaptive strategies. Quat. Int. 444 (Part B), 36–55. https://doi.org/10.1016/j.quaint.2017.02.034.

Provan, J., Bennett, K.D., 2008. Phylogeographic insights into cryptic glacial refugia. Trends Ecol. Evol. 23, 564–571. https://doi.org/10.1016/j.tree.2008.06.010.

R Development Core Team, 2016. R: A Language and Environment for Statistical Computing. R Foundation for Statistical Computing, Vienna.

Reimer, P.J., Austin, W.E., Bard, E., Bayliss, A., Blackwell, P.G., Ramsey, C.B., Butzin, M., Cheng, H., Edwards, R.L., Friedrich, M., Grootes, P.M., 2020. The IntCal20 Northern Hemisphere radiocarbon age calibration curve (0–55 cal kBP). Radiocarbon 62, 725–757. https://doi.org/10.1017/RDC.2020.41.

Reuther, J.D., Potter, B.A., Holmes, C.E., Feathers, J.K., Lanoe, F.B., Kielhofer, J., 2016. The rosa-keystone dunes field: the geoarchaeology and paleoecology of a late quaternary stabilized dune field in eastern Beringia. Holocene 26 (12), 1939–1953. https://doi.org/10.1177/0959683616646190.

Rijal, D.P., Heintzman, P.D., Lammers, Y., Yoccoz, N.G., Lorberau, K.E., Pitelkova, I., Goslar, T., Murguzur, F.J.A., Salonen, J.S., Helmens, K.F., Bakke, J., Edwards, M.E., Alm, T., Bråthen, K.A., Brown, A.G., Alsos, I.G., 2021. Sedimentary ancient DNA shows terrestrial plant richness continuously increased over the Holocene in northern Fennoscandia. Sci. Adv. 7, eabf9557 https://doi.org/10.1126/sciadv.abf9557.

Ritchie, J.C., 1984. Past and Present Vegetation of the Far Northwest of Canada. U. Toronto Press, Toronto, p. 272.

Ritchie, J.C., Cwynar, L.C., 1982. The late Quaternary vegetation of the north Yukon. In: Hopkins, D.M., Matthews Jr, J.V., Schweger, C.E., Young, S.B. (Eds.), Paleoecology of Beringia. Academic Press, New York, pp. 113–126.

Rowe, AG, Bataille, CP, Clement, P, Baleka, S, Combs, EA, Crass, BA, Fisher, DC, Ghosh, S, Holmes, CE, Krasinski, KE, Lanoë, F, Murchie, T, Poinar, H., Potter, B, Rasic, JT, Reuther, J, Smith, GM, Spaleta, KJ, Wygal, BT, Wooller, MJ., 2024. A female woolly mammoth's lifetime movements end in an ancient Alaskan hunter-gatherer camp. Sci 10, eadk0818.

Sjögren, Per, Edwards, Mary E., Gielly, Ludovic, Langdon, Catherine T., Croudace, Ian W., Merkel, Marie Kristine Føreid, Fonville, Thierry, Alsos, Inger Greve, 2017. Lake sedimentary DNA accurately records 20th Century introductions of exotic conifers in Scotland. In: New Phytologist (2016). https://doi.org/10.1111/nph.14199.

Soininen, E.M., Gauthier, G., Bilodeau, F., Berteaux, D., Gielly, L., Taberlet, P., Gussarova, G., Bellemain, E., Hassel, K., Stenøien, H.K., Epp, L., Schrøder-Nielsen, A., Brochmann, C., Yoccoz, N.G., 2015. Highly overlapping winter diet in two sympatric lemming species revealed by DNA metabarcoding. PLoS One 10, e0115335. https://doi.org/10.1371/journal.pone.0115335.

Sønstebo, J.H., Gielly, L., Brysting, A.K., Elven, R., Edwards, M., Haile, J., Willerslev, E., Coissac, E., Rioux, D., Sannier, J., Taberlet, P., Brochmann, C., 2010. Using next-generation sequencing for molecular reconstruction of past Arctic vegetation and climate. Mol. Ecol. Res. 10, 1009–1018. https://doi.org/10.1111/j.1755-0998.2010.02855.x.

Stewart, L., Alsos, I.G., Bay, C., Breen, A.L., Brochmann, C., Boulanger-Lapointe, N., Broennimann, O., Bültmann, H., Bøcher, P.K., Damgaard, C., Daniëls, F.J.A., Ehrich, D., Eidesen, P.B., Guisan, A., Jonsdottir, I.S., Lenoir, J., le Roux, P.C., Levesque, E., Luoto, M., Nabe-Nielsen, J., Schèonswetter, P., Tribsch, A., Tveraabak, L.U., Virtanen, R., Walker, D.A., Westergaard, K.B., Yoccoz, N.G., Svenning, J.-C., Wisz, M., Schmidt, N.M., Pellissier, L., 2016. The regional species richness and genetic diversity of Arctic vegetation reflect both past glaciations and current climate. Global Ecol. Biogeogr. 25, 430e442. https://doi.org/10.1111/geb.12424.

Stoof-Leichsenring, K.R., Huang, S., Liu, S., Jia, W., Li, K., Liu, X., Pestryakova, L., Herzschuh, U., 2022. Sedimentary DNA identifies modern and past macrophyte diversity and its environmental drivers in high-latitude and high-elevation lakes in Siberia and China. Limnol. Oceanogr. 67, 1126–1141. https://doi.org/10.1002/lno.12061.

Swanson, D.K., 2002. A comparison of taiga flora in north-eastern Russia and Alaska/Yukon. J. Biogeogr. 30, 1109–1121. https://doi.org/10.1046/j.1365-2699.2003.00901.x.

Taberlet, P., Coissac, E., Pompanon, F., Gielly, L., Miquel, C., Valentini, A., Vermat, T., Corthier, G., Brochmann, C., Willerslev, E., 2007. Power and limitations of the chloroplast trnL (UAA) intron for plant DNA barcoding. Nucleic Acids Res. 35, e14. https://doi.org/10.1093/nar/gkl938.

Tinner, W., Hu, F.S., Beer, R., Kaltenrieder, P., Scheurer, B., Krähenbühl, U., 2006. Postglacial vegetational and fire history: pollen, plant macrofossil and charcoal records from two Alaskan lakes. Veg. Hist. Archaeobotany 15 (4), 279–293. https://doi.org/10.1007/s00334-006-0052-z.

Viereck, L.A., Dyrness, C.T., Batten, A.R., Wenzlick, K.J., 1992. The Alaska Vegetation Classification. USDA Forest Service, Pacific Northwest Research Station. General Technical Report PNW-GTR-286.

Van Vierssen, W., 1982. The ecology of communities dominated by *Zannichellia* taxa in western Europe. II. Distribution, synecology and productivity aspects in relation to environmental factors. Aquat. Bot. 13, 385–483. https://doi.org/10.1016/0304-3770(82)90073-0.

Walker, D.A., Bockheim, J.G., Chapin, F.S.I.I.I., Eugster, W., Nelson, F.E., Ping, C.L., 2001. Calcium-rich tundra, wildlife, and the "mammoth steppe". Quat. Sci. Rev. 20 (1–3), 149–163. https://doi.org/10.1016/S0277-3791(00)00126-8.

Wang, Y., Heintzman, P.D., Newsom, L., Bigelow, N.H., Wooller, M.J., Shapiro, B., Williams, J.W., 2017. The southern coastal Beringian land bridge: cryptic refugium or pseudorefugium for woody plants during the Last Glacial Maximum? J. Biogeogr. 44, 1559–1571. https://doi.org/10.1111/jbi.13010.

Wang, Y., et al., 2021. Late Quaternary dynamics of Arctic biota from ancient environmental genomics. Nature 600, 86–92. https://doi.org/10.1038/s41586-021-04016-x.

Wesser, S.D., Armbruster, W.S., 1991. Species distribution controls across A forest-steppe transition: a causal model and experimental test. Ecol. Monogr. 61, 323–342. https://doi.org/10.2307/2937111.

Willerslev, E., et al., 2014. Fifty thousand years of Arctic vegetation and megafaunal diet. Nature 506, 47–51. https://doi.org/10.1038/nature12921.

WorldClimate, 2012. http://www.worldclimate.com/.

Wright Jr., H.E., 1967. A square-rod piston sampler for lake sediments. Journal ofSedimentary Petrology 37, 975–976.

Yoccoz, N.G., Bråthen, K.A., Gielly, L., Haile, J., Edwards, M.E., Goslar, T., von Stedingk, H., Brysting, A.K., Coissac, E., Pompanon, F., Sønstebø, J.H., Miquel, C., Valentini, A., de Bello, F., Chave, J., Thuiller, W., Wincker, P., Cruaud, C., Gavory, F., Rasmussen, M., Gilbert, M.T.P., Orlando, L., Brochmann, C., Willerslev, E., Taberlet, P., 2012. DNA from soil mirrors plant taxonomic and growth form diversity. Mol. Ecol. 21, 3647–3655.

Yurtsev, B.A., 2001. The Pleistocene "Tundra-Steppe" and the productivity paradox: the landscape approach. Quat. Sci. Rev. 20, 165–174. https://doi.org/10.1111/j.1365-294X.2012.05545.x.

Zazula, G.D., Froese, D.G., Elias, S.A., Kuzmina, S., La Farge, C., Reyes, A.V., Sanborn, P. T., Schweger, C.E., Smith, C.S., Mathewes, R.W., 2006a. Vegetation buried under Dawson tephra (25,300 14C years BP) and locally diverse late Pleistocene paleoenvironments of Goldbottom Creek, Yukon, Canada. Palaeogeogr. Palaeoclimatol. Palaeoecol. 242, 253–286. https://doi.org/10.1016/j.palaeo.2006.06.005.

Zazula, G.D., Telka, A.M., Harington, C.R., Schweger, C.E., Mathewes, R.W., 2006b. New spruce (*Picea* spp.) macrofossils from Yukon territory: implications for late Pleistocene refugia in eastern Beringia. Arctic 59, 391–400.

Zazula, G.D., Froese, D.G., Elias, S.A., Kuzmina, S., Mathewes, R.W., 2007. Arctic ground squirrels of the mammoth-steppe: paleoecology of Late Pleistocene middens (~24 000–29 450 14C yr BP), Yukon Territory, Canada. Quat. Sci. Rev. 26, 979–1003. https://doi.org/10.1016/j.quascirev.2006.12.006.

Zimmermann, H.H., Raschke, E., Epp, L.S., Stoof-Leichsenring, K.R., Schirrmeister, L., Schwamborn, G., Herzschuh, U., 2017. Sedimentary ancient DNA and pollen reveal the composition of plant organic matter in Late Quaternary permafrost sediments of the Buor Khaya Peninsula (north-eastern Siberia). Biogeosciences 14, 575–596. https://doi.org/10.5194/bg-14-575-2017.